Transverse momentum dependent parton distribution and fragmentation functions with QCD evolution

Aybat, S.M.; Rogers, T.C.

published in
Physical Review D
2011

DOI (link to publisher)
10.1103/PhysRevD.83.114042

document version
Publisher's PDF, also known as Version of record

PHYSICAL REVIEW D **83,** 114042 (2011)

Transverse momentum dependent parton distribution and fragmentation functions with QCD evolution

S. Mert Aybat[1,2,*] and Ted C. Rogers[2,†]

[1]*Nikhef Theory Group, Science Park 105, 1098XG Amsterdam, The Netherlands*
[2]*Department of Physics and Astronomy, Vrije Universiteit Amsterdam, NL-1081 HV Amsterdam, The Netherlands*
(Received 31 January 2011; published 23 June 2011)

We assess the current phenomenological status of transverse momentum dependent (TMD) parton distribution functions (PDFs) and fragmentation functions (FFs) and study the effect of consistently including perturbative QCD (pQCD) evolution. Our goal is to initiate the process of establishing reliable, QCD-evolved parametrizations for the TMD PDFs and TMD FFs that can be used both to test TMD factorization and to search for evidence of the breakdown of TMD factorization that is expected for certain processes. In this article, we focus on spin-independent processes because they provide the simplest illustration of the basic steps and can already be used in direct tests of TMD factorization. Our calculations are based on the Collins-Soper-Sterman (CSS) formalism, supplemented by recent theoretical developments which have clarified the precise definitions of the TMD PDFs and TMD FFs needed for a valid TMD-factorization theorem. Starting with these definitions, we numerically generate evolved TMD PDFs and TMD FFs using as input existing parametrizations for the collinear PDFs, collinear FFs, nonperturbative factors in the CSS factorization formalism, and recent fixed-scale fits. We confirm that evolution has important consequences, both qualitatively and quantitatively, and argue that it should be included in future phenomenological studies of TMD functions. Our analysis is also suggestive of extensions to processes that involve spin-dependent functions such as the Boer-Mulders, Sivers, or Collins functions, which we intend to pursue in future publications. At our website [http://projects.hepforge.org/tmd/], we have made available the tables and calculations needed to obtain the TMD parametrizations presented herein.

DOI: 10.1103/PhysRevD.83.114042 PACS numbers: 12.38.Bx, 12.39.St, 12.38.Cy, 12.20.Ds

I. INTRODUCTION

The factorization theorems of perturbative QCD (pQCD) have been instrumental in the successful application of QCD theory to phenomenology. The standard collinear factorization formalism [1] makes use of ''integrated'' parton distribution functions (PDFs) and fragmentation functions (FFs) which depend only on a single longitudinal momentum fraction, while the small momentum components, including the *transverse* components, are integrated over in the definitions. The integrated PDFs and FFs have consistent operator definitions in QCD, with appealing interpretations in terms of parton-model concepts. However, the standard collinear factorization formalism relies on approximations that are only valid for sufficiently inclusive observables. In order to address many of the issues now at the forefront of research in QCD and its role in hadron structure, pQCD factorization must be extended to situations where the usual approximations are not appropriate.

A transverse momentum dependent *(TMD)-factorization* formalism goes beyond the standard factorization framework by allowing the PDFs and FFs to depend on intrinsic transverse momentum in addition to the usual momentum fraction variables. As such, different sets of approximations are needed in the factorization proofs. The PDFs and FFs in a TMD-factorization formalism are referred to as TMD PDFs and TMD FFs (they are also called ''unintegrated'' or '' k_T dependent'') to distinguish them from the more familiar integrated correlation functions of collinear factorization. Henceforth, we will refer to TMD PDFs and TMD FFs collectively as ''TMDs.''

The role of the intrinsic transverse momentum carried by partons in high energy collisions is becoming increasingly central in discussions of how to probe the details of hadronic structure in high energy collisions. The usefulness of the TMD concept is evident from the large variety of situations where it makes an appearance. Generally, TMD factorization is needed to describe processes that are sensitive to intrinsic parton transverse momentum. The Drell-Yan (DY) process, single-inclusive deep inelastic scattering (SIDIS), and back-to-back hadron production in electron-positron annihilation at small transverse momentum are all classic examples of where TMD-factorization formulas are frequently used. More recently, TMD PDFs and FFs have been under intense study as objects that carry information about the spin structure of hadrons; the Boer-Mulders, Sivers, and pretzelosity functions are all specific examples of TMD PDFs, while the Collins function is an example of a TMD FF. For a recent review of TMDs in spin physics, see Ref. [2]. In very high

*maybat@nikhef.nl
†trogers@few.vu.nl

energy (small-x) resummation physics, where there is a lack of k_T ordering, the TMD gluon distribution is especially important, and similar issues must be dealt with. Finally, TMD functions are useful tools in the construction of Monte Carlo event generators, where the details of final state kinematics are of interest.

While TMDs can potentially provide a much deeper understanding of QCD and hadron structure, the theoretical framework of TMD factorization is much more complicated than the more standard collinear factorization. In derivations of collinear factorization, there are important cancellations that occur *after* integrations of parton momentum are carried out. With TMD factorization, the integrals over parton transverse momentum are left undone in the definitions of the TMDs, and contributions that would ordinarily cancel in a collinear factorization treatment must be accounted for. Collins, Soper, and Sterman (CSS) constructed a TMD-factorization formalism [3–5] that deals with the main complications of transverse momentum dependence, and provides a systematic treatment of pQCD over the full range of transverse momentum. The CSS formalism has proven highly successful in specific phenomenological applications such as in the calculation of the transverse momentum distributions in DY processes (see, for example, [6,7]), and is also well suited for the production of back-to-back particles in e^+e^- annihilation. The same methods are needed for the discovery of new particles like the standard model Higgs boson [8–10]. Furthermore, extensions of the CSS TMD-factorization formalism have been derived for SIDIS [11–13], and including spin in Ref. [14].

However, the most common methods for applying the CSS formalism are not ideally suited for studies that are specifically oriented toward understanding the TMD PDFs and TMD FFs themselves. Furthermore, the relationship between the full pQCD treatment of factorization and parton-model intuition has remained much less clear in TMD factorization than in collinear factorization. This has led to considerable confusion about how the study of TMDs should be approached in pQCD. That confusion is especially apparent from a comparison between current applications of TMD factorization and collinear factorization: While there have been extensive programs dedicated to parametrizing and evolving the integrated PDFs and FFs (making them indispensable and portable tools for phenomenology), a generally agreed upon framework for dealing with TMDs in an analogous way has not yet been established. More disturbingly, there has been a persistent lack of clarity or agreement regarding the definitions of the TMDs. A suitable set of definitions must be dictated by the requirements of factorization and universality, but the most common and naive definitions lead to inconsistencies, including unphysical divergences.

Over roughly the past decade, there has been steady progress toward a better understanding of what is needed [15–24]. The issue of finding the right definitions has now been especially brought into focus by the recent work of Collins [25,26]. The definitions for the TMDs in Ref. [25] are uniquely determined by the requirements of factorization, maximal universality, and internal consistency. (By ''maximal universality'' we mean that the same correlation functions appear in a large number of processes.) The confusion over definitions therefore appears to be solved. With the new definitions, the implementation of evolution via the CSS formalism is not modified significantly from earlier treatments which means that existing parametrizations of the nonperturbative parts can still be used. However, they can now be understood as contributions to separate, QCD-evolved TMDs. Moreover, as we will discuss in the next two sections, the new definitions have a much more direct relationship with more intuitive, parton-model based ways of viewing TMD factorization.

There has been much recent work devoted to parametrizing TMDs by assuming a parton-model picture of TMD factorization and directly fitting cross section calculations to experimental data [27–32]. This approach to TMD phenomenology is often called the *generalized parton model* (GPM) [33].

In addition, by working with nonperturbative models, it is possible to study the general properties of the TMDs and their relationships with each other. (See Ref. [34] and references therein for an overview of this subject.) A famous example is the illustration via model calculation that the Sivers function is nonvanishing in SIDIS [35,36].

However, most efforts to parametrize or model TMDs, particularly the spin-dependent TMDs, have ignored the role of evolution. For the unpolarized TMD PDFs there have been detailed implementations of evolution (e.g. [37,38]) However, even in the unpolarized case, the identification of the separate evolved TMDs and their relationship with the fundamental definitions in a complete treatment of factorization has remained unclear. The main purpose of the present article is to initiate the process of consistently including QCD evolution in parametrizations and models of TMDs by following the definitions in Ref. [25]. Addressing evolution is now an especially pressing task, given the very wide range of energy scales set to be probed in experiments in the near future, from Jefferson Lab (JLab) to the LHC. It has already been shown in Refs. [39,40] that evolution (in the form of Sudakov suppression) should be expected to be large. In our analysis, we will illustrate how this follows from the evolution of the individual TMDs. We also aim to facilitate the future implementation of evolution in studies of TMDs by clarifying the relationship between the parton-model description of TMD factorization and the CSS formalism. To this end, we have made computations available at [41] that illustrate how to obtain evolved TMDs given a choice of nonperturbative starting input.

An alternative approach to probing spin effect is to consider higher twist collinear functions such as the Qiu-Sterman function [42]. By taking transverse momentum moments of cross sections it is possible to relate TMDs to these higher twist functions [19]. See Ref. [43] for recent work on the evolution of weighted spin-dependent correlation functions.

Establishing reliable, evolved TMDs is also important for testing factorization and searching for instances of factorization breaking. Discussions of nonuniversality or factorization breaking often bring in the concept of Wilson lines (or gauge links), and the process dependent properties that can be associated with them. Already when comparing the Sivers function in SIDIS and the DY process, one must account for a well-known sign flip that is due to the reversed direction of the Wilson lines in these two processes [44]. More recently, it has been shown that obtaining consistent Wilson lines is even more problematic in the hadroproduction of hadrons or jets ($H_1 + H_2 \to H_3 + H_4 + X$). In such cases that require TMD factorization, it was found that *at a minimum* the Wilson lines for separate TMDs are highly complex and process dependent [45–47]. It was later shown in Ref. [48] that TMD factorization generally breaks down completely in the hadroproduction of hadrons. That is, separate TMDs cannot even be defined for each external hadron regardless of what Wilson lines are used in the definitions.

The complication in the case of the complete breakdown of factorization is caused by a failure of the usual gauge invariance/Ward identity arguments that are needed in a factorization proof. A confirmation of this effect would point to interesting new features of strong interaction physics, given that the breakdown of factorization is in just the range of kinematics where factorization would naively be expected to hold. Calculations in a GPM framework [49–51] will be needed for making predictions that can be compared with experiment to test factorization and/or search for factorization breaking. Furthermore, computations using the methods in, for example, Refs. [52–54], can potentially help to quantify and better understand the factorization breaking mechanism. It may soon be possible to find experimental evidence for factorization breaking, particularly in the analysis of RHIC data. (See, for example, the recent analysis of Refs. [55–58].) However, definitive tests of factorization or factorization breaking can only become possible with a more precise determination of the TMDs. Another motivation for this article is therefore to begin the determination of TMD parametrizations that should be used in tests of factorization in the case of spin-independent hadroproduction of back-to-back hadrons. Finally, in this paper we include some details of the calculation of the evolution of the TMD PDFs that did not appear in Ref. [25].

The paper is organized as follows: in Sec. II, a brief background of TMD factorization is provided, and the main complications that arise in the context of pQCD are discussed. In Sec. III, we set up the notation, and in Sec. IV we explain the definitions of TMD correlation functions. In Sec. V, we discuss the evolution of the TMDs in terms of the CSS formalism. We apply evolution to existing unpolarized quark TMD fits in Sec. VI, and we present some numerical results. We conclude with an overview and a discussion of future work in Sec. VII. In the appendices, we provide some details of the perturbative parts of our calculations.

II. THE DIFFERENT PICTURES OF TMD FACTORIZATION

In this section we expand on the general remarks in the Introduction by providing a very schematic overview of the different ways TMD factorization is approached in phenomenological applications. We discuss the relationship between parton-model intuition and full pQCD while emphasizing the complications that can arise. We explain the potential for confusion when evolution and soft factors are included, and how this is solved by the use of fully consistent definitions for the TMDs.

A. The generalized parton model

We start by considering the simplest parton-model picture of high energy collisions. There, the concept of a TMD-factorization formula becomes very intuitive and easy to state. The cross section is simply a partonic subprocess, folded with TMD PDFs and TMD FFs. In SIDIS, for example, the hadronic tensor is written as

$$W^{\mu\nu} = \sum_f |\mathcal{H}_f(Q)^2|^{\mu\nu} \times \int d^2\mathbf{k}_{1T} d^2\mathbf{k}_{2T} F_{f/p}(x, \mathbf{k}_{1T}) D_{h/f}(z, z\mathbf{k}_{2T}) \times \delta^{(2)}(\mathbf{k}_{1T} + \mathbf{q}_T - \mathbf{k}_{2T}). \quad (1)$$

Here $|\mathcal{H}_f(Q)^2|^{\mu\nu}$ describes the hard partonic subprocess, $\gamma^* q \to q$, for scattering off a quark of flavor f as a function of the hard scale Q. (It also includes any overall factors needed to make the left side a proper hadronic tensor.) The size of $\mathbf{q}_T$ is a measure of the noncollinearity in the process. Within the parton model, the TMDs $F_{f/p}(x, \mathbf{k}_{1T})$ and $D_{h/f}(z, z\mathbf{k}_{2T})$ have simple probabilistic interpretations; $F_{f/p}(x, \mathbf{k}_{1T})$, for example, is the probability density for finding a quark of flavor f with momentum fraction x and transverse momentum $\mathbf{k}_{1T}$ inside the proton. Equation (1) is closely analogous to the standard *collinear* factorization theorem of inclusive processes [59]. The only difference is that the TMD PDFs and FFs are allowed to carry intrinsic transverse momentum.

The intuitive approach to TMD factorization embodied by Eq. (1) forms the basis of much current TMD phenomenology. However, derivations of TMD factorization order by order in real pQCD involve complications that are not immediately apparent in parton-model reasoning. Indeed,

some aspects of partonic intuition can quickly lead to incorrect results if taken too literally. Furthermore, without a complete derivation of factorization, the issue of universality (or nonuniversality) of the TMDs in Eq. (1) is much less clear.

B. Divergences and soft factors

One issue is the appearance of extra divergences. In addition to the standard UV divergences associated with the renormalization of the theory, the TMD correlation functions also contain so-called ''light-cone'' divergences. They arise if the Wilson lines (gauge links) in the definitions of the TMDs point in exactly lightlike directions. We should note that the same light-cone singularities are not present in the ordinary collinear correlation functions because they cancel in a sum over final state interactions, which is possible due to integrations over the loop momenta, including the k_T integrals. Light-cone divergences correspond to gluons moving with infinite rapidity in the direction *opposite* the containing hadron, and are not regulated by the use of an infrared cutoff, so they amount to a real inconsistency in the definitions of TMDs. The most naive definitions, therefore, are invalid, and modifications are needed for a reliable factorization theorem. (See Refs. [20,24] and references therein for a review of this and other subtleties involved in defining consistent PDFs.) The light-cone divergences need to be regulated, typically by tilting the Wilson lines slightly away from the exactly lightlike directions.

Furthermore, in a TMD-factorization formula the role of soft gluons becomes important. (In this paper, ''soft'' refers to nearly on-shell gluons with rapidity intermediate between the rapidities of the colliding hadrons and produced jets.) They imply that another correlation function, a separate soft factor, should be inserted into factorization formulas like Eq. (1), in addition to the usual TMD PDFs and FFs. Already, the appearance of a soft factor seems to contradict the basic parton-model intuition.

The complications listed above, as well as a consistent matching to collinear factorization at large transverse momentum, are accounted for in the CSS formalism [3–5]. With the Wilson lines tilted to remove light-cone divergences, the factorization formula acquires new arbitrary parameters. Predictive power is then recovered by a kind of generalization of renormalization group techniques. The resulting evolution equations may be thought of as describing the variation of the TMDs and the soft factors with changes in the degree of tilt of the Wilson lines. Physically, this corresponds roughly to a variation with respect to a cutoff on the phase space available for recoil against soft gluons.

C. Confusion over TMD definitions

While the CSS formalism has been very useful for past phenomenological studies, the usual implementations bear little surface resemblance to the generalized partonic picture we started out with in Eq. (1). For example, in Ref. [38] (and similar applications of the CSS formalism to the DY process), the effects of evolution are gathered into separate factors, and it is not clear how they relate to separate TMD PDFs. In other treatments (e.g., [13,60]), factorization formulas for SIDIS are provided which contain explicit evolved TMDs, but they also involve separate explicit soft factors, and the hard part has explicit dependence on light-cone divergence cutoff parameters. Moreover, given the general observations that are reviewed in Refs. [20,24,61], it is questionable whether the most commonly quoted definitions of the TMDs are even fully consistent.

The original work of Collins and Soper [3] used a non-light-like axial gauge to regulate the rapidity divergences. Later, Collins and Hautmann [15,16,20] proposed definitions in which the main legs of the Wilson lines are lightlike, but in which there is a division by a special type of soft factor which cancels the rapidity divergences. However, these definitions continue to suffer from problems, including the appearance of badly divergent Wilson line self-energy contributions as discussed recently in Ref. [24] and also utilized in the treatment of TMD PDFs in Ref. [23]. While many of these issues have typically been discussed in the context of TMD PDFs, the same problems arise in the treatment of FFs.

Finally, it has remained unclear how the TMDs that have been used in past applications of evolution and the CSS formalism are related to the TMDs of other approaches, such as those based more on generalized parton-model pictures. In parametrizations of TMDs, the role of the soft factor is often not explicitly included and evolution is ignored. Many other theoretical TMD studies continue to quote definitions with exactly lightlike Wilson lines. Knowledge of the operator definitions for the TMDs is also needed for lattice TMD calculations [62,63], and in model calculations. Clearly, a more unified treatment of TMD factorization is necessary in order to bring together these different approaches to the study of TMDs.

D. Consistent definitions, TMD factorization, and evolution

What is needed, in addition to fully consistent TMD definitions, is a formulation that retains as much as possible the basic factorized structure of Eq. (1), but which appropriately includes evolution and the effects of soft factors. Ideally, the situation should be closely analogous to what already exists for collinear factorization. Namely, it should be possible to clearly identify consistent and universal TMDs that can be tabulated or parametrized and then reused in formulas like Eq. (1) to make predictions for a wide variety of processes. Fortunately, this has been achieved in the recent work of Ref. [25]. There, the factorization formula for SIDIS takes the form

$$W^{\mu\nu} = \sum_f |\mathcal{H}_f(Q;\mu)^2|^{\mu\nu} \times \int d^2\mathbf{k}_{1T} d^2\mathbf{k}_{2T} F_{f/p}(x, \mathbf{k}_{1T}; \mu; \zeta_F) \times D_{h/f}(z, z\mathbf{k}_{2T}; \mu; \zeta_D)\delta^{(2)}(\mathbf{k}_{1T} + \mathbf{q}_T - \mathbf{k}_{2T}) + Y(Q, \mathbf{q}_T) + \mathcal{O}((\Lambda/Q)^a). \quad (2)$$

The first term on the right-hand side of this equation (responsible for the low-$\mathbf{q}_T$ behavior) has exactly the structure of the partonic TMD-factorization formula in Eq. (1), apart from the scale dependence denoted by μ, ζ_F, and ζ_D. The arguments ζ_F and ζ_D will be discussed more in the explanation of the TMD definitions in Sec. IV. They are left over from the need to regulate light-cone divergences, and should obey $\sqrt{\zeta_F\zeta_D} \sim \mathcal{O}(Q^2)$. In terms of more familiar variables, they are defined as

$$\zeta_F = 2M_p^2 x^2 e^{2(y_P - y_s)} \quad (3)$$

and

$$\zeta_D = 2(M_H^2/z^2)e^{2(y_s - y_h)}. \quad (4)$$

Here, x and z are the usual Bjorken scaling and fragmentation variables, M_p is the proton mass, and M_h is the mass of the produced hadron. The rapidities of the proton and produced hadron are y_p and y_h, respectively. The rapidity y_s is an arbitrary low-rapidity cutoff parameter that separates partons with large forward rapidity (in the proton direction) from backward rapidity (in the produced hadron direction). Variations of these functions with y_s will be determined by the evolution equations.

The scale μ is the standard renormalization group (RG) scale. The TMD correlation functions, $F_{f/p}(x, \mathbf{k}_{1T}; \mu; \zeta_F)$ and $D_{h/f}(z, z\mathbf{k}_{2T}; \mu; \zeta_D)$, have definite and consistent operator definitions. They include the effects from soft gluons in such a way that no soft factor appears explicitly in Eq. (2). Evolution can be implemented on $F_{f/p}(x, \mathbf{k}_{1T}; \mu; \zeta_F)$ and $D_{h/f}(z, z\mathbf{k}_{2T}; \mu; \zeta_D)$ independently, and the basic steps closely follow the usual CSS approach. We will discuss the definitions more in the next section, but for now we mention that they solve most of the theoretical problems summarized in Refs. [20,24] and Sec. II C, including the appearance of light-cone divergences and Wilson line self-interactions.

The term $Y(Q, q_T)$ accounts for the large-$\mathbf{q}_T$ dependence of the cross section, where the approximations needed for TMD factorization break down. There, collinear factorization becomes the appropriate framework. The error term is suppressed by $(\Lambda/Q)^a$ where $a > 0$. The first term on the right side of Eq. (2) is valid up to corrections of order $(q_T/Q)^a$, but the $Y(Q, \mathbf{q}_T)$ is needed for a valid treatment of factorization over the full range of $\mathbf{q}_T$.

The derivation of Eq. (2) within pQCD factorization, with consistent definitions for the TMDs, is an important breakthrough because it connects TMD studies from a GPM framework with formal QCD and clarifies the meaning of TMD evolution. We will use Eq. (2), along with the associated definitions for the TMDs from Ref. [25] to obtain momentum-space fits for use in phenomenology. The nonperturbative input can be obtained from already existing models or fits made at fixed scales. For the TMD PDFs, much information about the nonperturbative input is already available from fits that use the standard $\mathbf{b}_T$-space formulation of the CSS formalism in the DY process.

III. SETUP AND NOTATION

We start by setting up the basic notation. In our convention for light-cone variables, a four-vector $V^\mu = (V^+, V^-, \mathbf{V}_T)$ has components

$$V^\pm = \frac{V^0 \pm V^z}{\sqrt{2}} \qquad \mathbf{V}_T = (V^x, V^y). \quad (5)$$

The z component picks out the forward direction. Note that $V^2 = 2V^+V^- - \mathbf{V}_T^2$.

For the processes we are interested in, there are always two relevant lightlike directions which we label u_A and u_B and define to be

$$u_A = (1, 0, \mathbf{0}_t) \qquad u_B = (0, 1, \mathbf{0}_t). \quad (6)$$

In the SIDIS example, u_A and u_B characterize the directions of the incoming proton and the produced jet. A Wilson line from a coordinate x to ∞ along the direction of a four-vector n is defined as usual:

$$W(\infty, x; n) = P\exp\left[-ig_0 \int_0^\infty ds n \cdot A_0^a(x + sn)t^a\right]. \quad (7)$$

In these definitions, the bare fields and couplings are used, P is a path-ordering operator, and t^a is the generator for the gauge group in the fundamental representation, with color index a.

As discussed in the previous section, light-cone divergences must be regulated by tilting the direction of the Wilson line away from the exactly lightlike direction. Therefore, we need to define another set of vectors n_A and n_B analogous to Eq. (6) but slightly tilted, so that they have rapidities y_A and y_B:

$$n_A = (1, -e^{-2y_A}, \mathbf{0}_t) \qquad n_B = (-e^{2y_B}, 1, \mathbf{0}_t). \quad (8)$$

Note that the tilted Wilson line directions are spacelike, $n_A^2 = n_B^2 < 0$. The use of spacelike directions for the Wilson lines ensures maximum universality for the definitions of the TMDs, as explained in Ref. [64]. In all of our calculations, μ is the standard $\overline{\text{MS}}$ mass scale in dimensional regularization and the dimensional regularization parameter ϵ is defined in the standard way as $2\epsilon = 4 - d$, where d is the dimension of space-time.

Though our results apply generally to the standard factorizable processes, we will continue to use SIDIS as a reference process for explaining the definitions. Let us

also rewrite the TMD-factorization formula for SIDIS in Eq. (2) as

$$\begin{aligned} W^{\mu\nu} &= \sum_f |\mathcal{H}_f(Q;\mu)^2|^{\mu\nu} \\ &\quad \times \int d^2\mathbf{k}_{1T} d^2\mathbf{k}_{2T} \delta^{(2)}(\mathbf{k}_{1T} + \mathbf{q}_T - \mathbf{k}_{2T}) \\ &\quad \times F_{f/p}(x, \mathbf{k}_{1T}; \mu; \zeta_F) D_{h/f}(z, z\mathbf{k}_{2T}; \mu; \zeta_D) \\ &= \sum_f |\mathcal{H}_f(Q;\mu)^2|^{\mu\nu} \int \frac{d^2\mathbf{b}_T}{(2\pi)^2} e^{-i\mathbf{q}_T\cdot\mathbf{b}_T} \\ &\quad \times \tilde{F}_{f/p}(x, \mathbf{b}_T; \mu; \zeta_F) \tilde{D}_{h/f}(z, \mathbf{b}_T; \mu; \zeta_D). \end{aligned} \tag{9}$$

Throughout this paper, it will be implicit that all momentum components are in the hadron frame. (The hadron frame is where both hadrons have zero transverse momentum and is a natural frame for setting up the steps for factorization.)

Hereafter, the $Y(Q, \mathbf{q}_T)$ term that appeared in Eq. (2) will also be dropped because our primary interest is in the $q_T \ll Q$ regime where TMD factorization is appropriate. Also, we will drop any explicit $+\mathcal{O}((\Lambda/Q)^a)$ symbols. We have written the TMD-factorization formula in coordinate space in the second equation of (9) because it is simpler to explain the coordinate space definitions of the TMDs and their evolution. Later we will Fourier transform the TMDs back to momentum space when we analyze them numerically.

IV. DEFINITIONS OF THE TMDS

As explained in Sec. II, our calculations are based on the formulation of TMD factorization explained in detail in Ref. [25]. A repeat of the derivation is beyond the scope of this paper. However, in order to put our later calculations into their proper context, we will give an overview of the basic features of the formalism in this and the next section. We refer the reader directly to Ref. [25] for pertinent details.

A. Soft-factor definition

We have already stressed in Sec. II C that the definitions of the TMDs in Eq. (9) are not the often quoted matrix elements of the form $\sim\langle P|\bar{\psi}$ Wilson line $\psi|P\rangle$ with simple lightlike Wilson lines connecting the field operators. Using such definitions in a factorization formula leads to inconsistencies, including unregulated light-cone divergences. Also, soft gluons with rapidity intermediate between the two nearly lightlike directions need to be accounted for in the form of soft factors. Therefore, before we can discuss the definitions of the TMDs that will ultimately be used in Eq. (9), we must provide the precise definition of the soft factor. In coordinate space it is an expectation value of a Wilson loop:

$$\begin{aligned} \tilde{S}_{(0)}(\mathbf{b}_T; y_A, y_B) &= \frac{1}{N_c} \langle 0| W(\mathbf{b}_T/2, \infty; n_B)^\dagger_{ca} \\ &\quad \times W(\mathbf{b}_T/2, \infty; n_A)_{ad} W(-\mathbf{b}_T/2, \infty; n_B)_{bc} \\ &\quad \times W(-\mathbf{b}_T/2, \infty; n_A)^\dagger_{db} |0\rangle_{\text{No S.I.}}. \end{aligned} \tag{10}$$

We have used the vectors in Eq. (8) to define the directions of the Wilson lines so that, as long as y_A and y_B are finite, the Wilson lines in Eq. (10) are non-light-like. The subscripts a, b, c, and d are color triplet indices, and repeated indices are summed over. The "(0)" subscript indicates that bare fields are used. The soft factor contains Wilson line self-interaction (S.I.) divergences that are very badly divergent and are unrelated to the original unfactorized graphs. They must therefore be excluded, and we indicate this with a subscript "No S. I.". We emphasize, however, that this is only a temporary requirement because all Wilson line self-energy contributions will cancel in the final definitions. Another potential complication, pointed out in Refs. [18,19], is that exact gauge invariance requires the Wilson lines to be closed by the insertion of links at light-cone infinity in the transverse direction. However, the transverse segments will not contribute in the final definitions of the TMDs (at least in nonsingular gauges), so we do not show them explicitly in Eq. (10). Again, the final arrangement of soft factors will ensure a cancellation.

Rather than appearing as a separate factor in the TMD-factorization formula, soft factors like Eq. (10) will be part of the final definitions of the TMDs. Their role in the definitions will be essential for the internal consistency of the TMDs and their validity in a factorization formula like Eq. (9).

B. TMD PDF and FF definitions

Now we turn to the definitions of the TMDs themselves, starting with the unpolarized TMD PDF. The most natural first attempt at an operator definition is obtained simply by direct extension of the collinear integrated parton distribution, though with the Wilson line tilted to avoid light-cone singularities. The operator definition is

$$\begin{aligned} &\tilde{F}^{\text{unsub}}_{f/P}(x, \mathbf{b}_T; \mu; y_P - y_B) \\ &= \text{Tr}_C \text{Tr}_D \int \frac{dw^-}{2\pi} e^{-ixP^+w^-} \langle P| \bar{\psi}_f(w/2) W(w/2, \infty, n_B)^\dagger \\ &\quad \times \frac{\gamma^+}{2} W(-w/2, \infty, n_B) \psi_f(-w/2) |P\rangle_{c,\text{No S.I.}}. \end{aligned} \tag{11}$$

This definition does not account for the overlap of the soft and collinear regions, so we refer to it as the "unsubtracted" TMD PDF. Here $w = (0, w^-, \mathbf{b}_T)$ and y_P is the physical rapidity of the hadron. As usual, the struck quark has a longitudinal plus-component of momentum $k^+ \equiv xP^+$. The non-light-like direction of the Wilson line is given by the n_B vector defined in Eq. (8) so that the light-cone divergences are regulated by the finite rapidity

y_B. As usual, the definition includes a trace over color. The c subscript is to indicate that only connected diagrams are included. Equation (11) reduces exactly to the most naive definition of the TMD PDF when the lightlike limit of $y_B \to -\infty$ is taken. Indeed, in the final definition we will take this limit, but then the role of the soft factors becomes important.

While the definition in Eq. (11) is intuitively appealing, modifications are needed in order to have a consistent definition that can be used in a factorization formula like Eq. (9). The complete definition for a quark f in proton P, given in Refs. [25,26], is

$$\tilde{F}_{f/P}(x, \mathbf{b}_T; \mu; \zeta_F) = \tilde{F}^{\text{unsub}}_{f/P}(x, \mathbf{b}_T; \mu; y_P - (-\infty)) \times \sqrt{\frac{\tilde{S}_{(0)}(\mathbf{b}_T; +\infty, y_s)}{\tilde{S}_{(0)}(\mathbf{b}_T; +\infty, -\infty)\tilde{S}_{(0)}(\mathbf{b}_T; y_s, -\infty)}} Z_F Z_2. \quad (12)$$

Here, the "∞" arguments for the rapidity variables in the unsubtracted PDF and the soft factors are meant in the sense of a limit. All field operators are unrenormalized, and Z_F and Z_2 are the PDF and field strength renormalization factors, respectively. The soft factors on the right-hand side of Eq. (12) contain rapidity arguments y_s. It is an arbitrary parameter which can be thought of as separating the extreme plus and minus directions. It will be convenient to express the dependence on y_s via ζ_F, defined in Eq. (3). On the left-hand side of Eq. (12), the dependence on y_s is expressed via the dependence on ζ_F.

Although we will not repeat the derivation that leads to Eq. (12), we remark that the definition is unique given the requirements that: (a) Factorization holds with maximal universality for the TMDs. (b) No explicit soft factor appears in the final factorization formula, Eq. (9). (c) Self-interactions of the Wilson lines, and attachments to gauge links at infinity cancel in the final definition. (d) The Collins-Soper (CS) equations are homogeneous.

There is an analogous definition for the TMD FF. The unsubtracted version, analogous to Eq. (11), is

$$\tilde{D}^{\text{unsub}}_{H/f}(z, \mathbf{b}_T; \mu; y_A - y_h) = \sum_X \frac{1}{4N_{c,f}} \text{Tr}_C \text{Tr}_D \frac{1}{z} \int \frac{dw^-}{2\pi} e^{ik^+ w^-} \langle 0 | \gamma^+ W(w/2, \infty, n_A) \times \psi_f(w/2) | h, X \rangle \langle h, X | \bar{\psi}_f(-w/2) \times W(-w/2, \infty, n_A)^\dagger | 0 \rangle_{c,\text{No S.I.}}. \quad (13)$$

Now y_h is the physical rapidity of the produced hadron or jet. The complete definition of the TMD FF with the soft factors included is

$$\tilde{D}_{H/f}(z, \mathbf{b}_T; \mu; \zeta_D) = \tilde{D}^{\text{unsub}}_{H/f}(z, \mathbf{b}_T; \mu; +\infty - y_h) \times \sqrt{\frac{\tilde{S}_{(0)}(\mathbf{b}_T; y_s, -\infty)}{\tilde{S}_{(0)}(\mathbf{b}_T; +\infty, -\infty)\tilde{S}_{(0)}(\mathbf{b}_T; +\infty, y_s)}} Z_D Z_2. \quad (14)$$

Again there is dependence on the soft rapidity y_s. For the FF, the energy cutoff scale ζ_D is related to the soft rapidity scale y_s via Eq. (4).

Equations (12) and (14) are the correct TMDs for the TMD-factorization formula in Eq. (9) as well as for e^+e^- annihilation with back-to-back jets. Up to a flip in the direction of the Wilson line from future to past pointing, which is important for accounting for a sign flip in certain types of TMDs, the TMD PDF in (12) is also relevant for the Drell-Yan process. In this section we have clarified the meaning of the energy parameters ζ_F and ζ_D, which were already discussed in Secs. II and III. Together, Eqs. (3) and (4) give $\sqrt{\zeta_F \zeta_D} \approx Q^2$. They are in principle arbitrary, and the full factorization formula in Eq. (9) is exactly independent of the choice of y_s (and therefore $\sqrt{\zeta_F}$ and $\sqrt{\zeta_D}$). However, different choices are needed for each factor in Eq. (9) in order to optimize the convergence properties of the perturbation series. To obtain the TMDs appropriate for different scales, we must appeal to evolution equations which are the subject of Sec. V.

C. The role of soft factors

Admittedly, the final definitions in Eqs. (12) and (14) appear rather complex. While detailed derivations are beyond the scope of this paper, it is nevertheless worthwhile to make a few intuitive remarks about how these definitions arise in a treatment of factorization. A much more detailed treatment is found in Ref. [25].

For now we simplify the notation for the TMDs by dropping all arguments and symbols not directly related to Wilson line rapidities. The cross section can then be written (schematically) as

$$d\sigma = |\mathcal{H}|^2 \frac{\tilde{F}^{\text{unsub}}(y_P - (-\infty)) \times \tilde{D}^{\text{unsub}}(+\infty - y_h)}{\tilde{S}(+\infty, -\infty)}. \quad (15)$$

The $\tilde{F}^{\text{unsub}}(y_P - (-\infty))$ and $\tilde{D}^{\text{unsub}}(+\infty - y_h)$ are the same unsubtracted TMDs from Eqs. (11) and (13). They each describe the distribution of gluons in their relevant collinear direction, but they also both account for soft gluons with nearly zero rapidity. Therefore, the soft factor $\tilde{S}(+\infty, -\infty)$ in the denominator is needed to remove double counting. Since the Wilson lines in the unsubtracted TMDs are lightlike in the plus and minus directions, respectively, they also include rapidity divergences. Thus, the role of the $\tilde{S}(+\infty, -\infty)$ is also to cancel these rapidity divergences. Although Eq. (15) properly accounts for all

soft and collinear regions and deals with the divergences, it is not factorized. Because of the rapidity divergences, it is immediately clear that $\tilde{F}^{\text{unsub}}(y_P - (-\infty))$ and $\tilde{D}^{\text{unsub}}(+\infty - y_h)$ are not separately well defined, and in the full formula they are entangled via the soft denominator. To get a factorized structure for Eq. (15), with each factor individually well defined, a natural first step to try is simply to separate the soft factor into a product of two factors:

$$d\sigma = |\mathcal{H}|^2 \frac{\tilde{F}^{\text{unsub}}(y_P - (-\infty))}{\sqrt{\tilde{S}(+\infty, -\infty)}} \frac{\tilde{D}^{\text{unsub}}(+\infty - y_h)}{\sqrt{\tilde{S}(+\infty, -\infty)}}. \quad (16)$$

One is then tempted to identify the factors on either side of the "×" with the TMD PDF and the TMD FF. However, these definitions still contain uncanceled divergences. In each factor, the rapidity divergence in the numerator is not completely canceled by the square root rapidity divergence in the denominator, and new rapidity divergences are introduced by the Wilson line pointing in the opposite direction. So the next modification of Eq. (15) is to write

$$\begin{aligned} d\sigma &= |\mathcal{H}|^2 \frac{\tilde{F}^{\text{unsub}}(y_P - (-\infty))}{\sqrt{\tilde{S}(+\infty, -\infty)}} \frac{\sqrt{\tilde{S}(+\infty, -\infty)}}{\sqrt{\tilde{S}(+\infty, -\infty)}} \\ &\quad \times \frac{\tilde{D}^{\text{unsub}}(+\infty - y_h)}{\sqrt{\tilde{S}(+\infty, -\infty)}} \\ &= |\mathcal{H}|^2 \frac{\tilde{F}^{\text{unsub}}(y_P - (-\infty))}{\sqrt{\tilde{S}(+\infty, -\infty)}} \frac{\sqrt{\tilde{S}(+\infty, y_s)\tilde{S}(y_s, -\infty)}}{\sqrt{\tilde{S}(+\infty, y_s)\tilde{S}(y_s, -\infty)}} \\ &\quad \times \frac{\tilde{D}^{\text{unsub}}(+\infty - y_h)}{\sqrt{\tilde{S}(+\infty, -\infty)}} \\ &= |\mathcal{H}|^2 \left\{ \tilde{F}^{\text{unsub}}(y_P - (-\infty)) \sqrt{\frac{\tilde{S}(+\infty, y_s)}{\tilde{S}(+\infty, -\infty)\tilde{S}(y_s, -\infty)}} \right\} \\ &\quad \times \left\{ \tilde{D}^{\text{unsub}}(+\infty - y_h) \sqrt{\frac{\tilde{S}(y_s, -\infty)}{\tilde{S}(+\infty, -\infty)\tilde{S}(+\infty, y_s)}} \right\}. \end{aligned} \quad (17)$$

After the first equality, we have simply multiplied and divided by $\sqrt{\tilde{S}(+\infty, -\infty)}$. After the second equality, we have used the group relation $\tilde{S}(y_A, y_C) \propto \tilde{S}(y_A, y_B)\tilde{S}(y_B, y_C)$, which follows from the evolution equations for the soft factor—see, e.g., Ref. [25], Chapter 10. [In fact, this expression should also include an overall factor that depends on rapidity y_B. But this cancels in Eq. (17) between the numerator and denominator and does not affect our argument.] This allows for a separation of the soft factors into pieces that have rapidity divergences only in the plus or only in the minus directions, with any other rapidity divergences cut off by the arbitrary scale y_s. By rearranging the soft factors, everything can then be grouped into the factors on the last two lines. In each factor, all spurious divergences cancel, and we arrive at the separately well-defined TMDs in braces. These correspond to the definitions in Eqs. (12) and (14).

To summarize, the lightlike Wilson lines are needed in each separate unsubtracted TMD of Eq. (15), but the contribution from gluon attachments to a Wilson line where the gluon has nearly the *same rapidity* as the Wilson line does not correspond to any real physics. To cancel these spurious contributions to the cross section, there must be an equal number of both plus-pointing and minus-pointing lightlike Wilson lines in the numerator and denominator, as is the case in Eq. (15). Applying this same requirement to the separate TMDs (a TMD PDF and a TMD FF, in our case) leads uniquely to the definition in the last two lines of Eq. (17) and Eqs. (12) and (14). Compare this with the situation in Ref. [65]. There, as in our Eq. (15), the needed cancellations occur in the full cross section expression, but not in the individual TMD factors. To get separately consistent TMDs, the steps summarized in Eq. (17) are needed.

V. EVOLVED TMDS

The evolution of the TMDs follows from their definitions, Eqs. (12) and (14). We start with the evolution of the TMD PDF. The energy evolution is given by the CS equation for Eq. (8):

$$\frac{\partial \ln \tilde{F}(x, \mathbf{b}_T; \mu, \zeta_F)}{\partial \ln \sqrt{\zeta_F}} = \tilde{K}(\mathbf{b}_T; \mu), \quad (18)$$

where the function $\tilde{K}(\mathbf{b}_T; \mu)$ is defined as

$$\tilde{K}(\mathbf{b}_T; \mu) = \frac{1}{2} \frac{\partial}{\partial y_s} \ln\left(\frac{\tilde{S}(\mathbf{b}_T; y_s, -\infty)}{\tilde{S}(\mathbf{b}_T; +\infty, y_s)} \right). \quad (19)$$

Equation (18) follows directly from differentiating Eq. (12) with respect to $\sqrt{\zeta_F}$ and using the definition of $\tilde{K}(\mathbf{b}_T; \mu)$. Note that it is $\tilde{S}(\mathbf{b}_T)$ rather than $\tilde{S}_{(0)}(\mathbf{b}_T)$ that appears in Eq. (19). Thus, it is important to account for the UV renormalization factors $Z_F Z_2$ in Eq. (12).

The RG equations for both $\tilde{F}(x, \mathbf{b}_T; \mu; \zeta_F)$ and $\tilde{K}(\mathbf{b}_T; \mu)$ are also needed. They are

$$\frac{d\tilde{K}(\mathbf{b}_T; \mu)}{d \ln \mu} = -\gamma_K(g(\mu)) \quad (20)$$

and

$$\frac{d \ln \tilde{F}(x, \mathbf{b}_T; \mu, \zeta_F)}{d \ln \mu} = \gamma_F(g(\mu); \zeta_F/\mu^2). \quad (21)$$

The functions $\gamma_K(g(\mu))$ and $\gamma_F(g(\mu); \zeta_F/\mu^2)$ are the anomalous dimensions of $\tilde{K}(\mathbf{b}_T; \mu)$ and $\tilde{F}(x, \mathbf{b}_T; \mu, \zeta_F)$,

respectively. Using Eqs. (18)–(21), the energy evolution of γ_F can be derived:

$$\gamma_F(g(\mu);\zeta_F/\mu^2) = \gamma_F(g(\mu);1) - \frac{1}{2}\gamma_K(g(\mu))\ln\frac{\zeta_F}{\mu^2}. \tag{22}$$

At small-b_T, Eq. (12) can itself be calculated within a collinear factorization formalism [3]. Namely, it separates into a perturbatively calculable hard scattering coefficient and an integrated PDF, convoluted over momentum fraction:

$$\tilde{F}_{f/P}(x,\mathbf{b}_T;\mu,\zeta_F) = \sum_j \int_x^1 \frac{d\hat{x}}{\hat{x}} \tilde{C}_{f/j}(x/\hat{x},b_T;\zeta_F,\mu,g(\mu)) f_{j/P}(\hat{x};\mu) + \mathcal{O}((\Lambda_{\rm QCD}b_T)^a). \tag{23}$$

The functions $f_{j/P}(\hat{x};\mu)$ are the ordinary integrated PDFs and the $\tilde{C}_{f/j}(x/\hat{x},b_T;\zeta_F,\mu,g(\mu))$ are the hard coefficient functions, which are provided to first order in Appendix A. The last term denotes the error, which grows large when $b_T \gtrsim \Lambda_{\rm QCD}^{-1}$.

At large b_T, the perturbative treatment of the b_T dependence is no longer reliable. In momentum space, this corresponds to the breakdown of the perturbative treatment of the k_T dependence at small k_T. It is in this region that the concept of TMD factorization, incorporating TMDs with intrinsic nonperturbative transverse momentum, becomes very important.

While the b_T dependence at large b_T cannot be calculated directly in pQCD, the scale dependence can still be handled with the evolution equations (18)–(22). But a prescription is needed for matching the large and small b_T behavior. The most common matching procedure was developed in Ref. [66]. It replaces $\mathbf{b}_T$ in the hard part of the calculation by a function,

$$\mathbf{b}_*(\mathbf{b}_T) \equiv \frac{\mathbf{b}_T}{\sqrt{1+b_T^2/b_{\rm max}^2}}. \tag{24}$$

This definition of $\mathbf{b}_*(\mathbf{b}_T)$ is constructed so that it is equal to $\mathbf{b}_T$ when $\mathbf{b}_T$ is small, while smoothly approaching an upper cutoff $b_{\rm max}$ when $\mathbf{b}_T$ becomes too large. The value of $b_{\rm max}$ is typically chosen to be of order $\sim 1\ {\rm GeV}^{-1}$ and should be thought of as characterizing the boundary of the perturbative region of the $\mathbf{b}_T$ dependence.

In the calculation of the hard coefficient in Eq. (23), the appropriate size for the scale μ is determined by the size of $\mathbf{b}_*(\mathbf{b}_T)$. Hence, we define the scale,

$$\mu_b = \frac{C_1}{b_*(\mathbf{b}_T)}. \tag{25}$$

The parameter C_1 is chosen to optimize the perturbation expansion. For all our calculations, we will use $C_1 = 2e^{-\gamma_E}$. At large b_T in the final expression for the evolved TMD PDF, the effect of the deviation between $\mathbf{b}_T$ and $\mathbf{b}_*$ in $\tilde{F}_{f/P}(x,\mathbf{b}_T;\mu;\zeta_F)$ and $\tilde{K}(\mathbf{b}_T;\mu)$ will be accounted for by extra nonperturbative, but universal and scale-independent, functions.

Applying the evolution equations in Eqs. (18)–(22), using the collinear factorization treatment for small $\mathbf{b}_T$ from Eq. (23), and implementing the matching procedure of Eq. (24) allows the TMD PDF to be written with maximum perturbative input in terms of evolution from fixed starting scales:

$$\tilde{F}_{f/P}(x,\mathbf{b}_T;\mu,\zeta_F) = \overbrace{\sum_j \int_x^1 \frac{d\hat{x}}{\hat{x}} \tilde{C}_{f/j}(x/\hat{x},b_*;\mu_b^2,\mu_b,g(\mu_b)) f_{j/P}(\hat{x},\mu_b)}^{A} \times \overbrace{\exp\left\{\ln\frac{\sqrt{\zeta_F}}{\mu_b}\tilde{K}(b_*;\mu_b) + \int_{\mu_b}^{\mu}\frac{d\mu'}{\mu'}\left[\gamma_F(g(\mu');1) - \ln\frac{\sqrt{\zeta_F}}{\mu'}\gamma_K(g(\mu'))\right]\right\}}^{B} \times \overbrace{\exp\left\{g_{j/P}(x,b_T) + g_K(b_T)\ln\frac{\sqrt{\zeta_F}}{\sqrt{\zeta_{F,0}}}\right\}}^{C}, \tag{26}$$

This is our master equation for fitting TMD PDFs while incorporating evolution. For a much more detailed explanation of the steps summarized above and leading to Eq. (26), we again refer the reader to Ref. [25], especially Chapters 10 and 13. The steps for evolving are very similar to traditional applications of the CSS formalism, but now they are applied to separate, individual TMDs. The scales used in the evolution are chosen to minimize the size of higher order corrections in the perturbatively calculable parts. We have labeled three separate factors by "A," "B," and "C" to aid in the detailed discussion that will appear in the next section. The $\tilde{C}_{f/j}(x/\hat{x},b_*;\mu_b^2,\mu_b,g(\mu_b))$, $\tilde{K}(b_*;\mu_b)$, $\gamma_F(g(\mu');1)$, and $\gamma_K(g(\mu'))$ functions are all perturbatively calculable for all $\mathbf{b}_T$. They are provided to order α_s in Appendices A and B. On the first line, $f_{j/P}(\hat{x},\mu_b)$ is the ordinary integrated PDF from collinear

factorization. The functions $g_{j/P}(x, b_T)$ and $g_K(b_T)$ describe the nonperturbative $\mathbf{b}_T$ behavior in $\tilde{F}_{f/P}(x, \mathbf{b}_T; \mu; \zeta_F)$ and $\tilde{K}(\mathbf{b}_T; \mu)$, respectively. They are scale independent and universal. The function $g_K(b_T)$ is notably independent of the species of external hadrons. Our definition of the factor $g_{j/P}(x, b_T)$ differs slightly from what is used in [25] because it has absorbed a term equal to $g_K(b_T)\ln(\sqrt{\zeta_{F,0}}/xM_p)$. This will allow us to choose an arbitrary starting scale $\zeta_{F,0}$ for the evolution in $\sqrt{\zeta_F}$.

We are ultimately interested in the momentum-space TMD which is just the Fourier transform of the coordinate space TMD PDF in Eqs. (12) and (26),

$$F_{f/P}(x, \mathbf{k}_T; \mu, \zeta_F) = \frac{1}{(2\pi)^2}\int d^2\mathbf{b}_T e^{i\mathbf{k}_T\cdot\mathbf{b}_T} \times \tilde{F}_{f/P}(x, \mathbf{b}_T; \mu, \zeta_F). \quad (27)$$

Once Eq. (26) has been parametrized, $F_{f/P}(x, \mathbf{k}_T; \mu, \zeta_F)$ can be determined directly by a numerical Fourier transform.

Exactly analogous steps hold for the TMD FF. It is related to $\tilde{K}(\mathbf{b}_T; \mu)$ by

$$\frac{\partial \ln\tilde{D}(z, \mathbf{b}_T; \mu, \zeta_D)}{\partial \ln\sqrt{\zeta_D}} = \tilde{K}(\mathbf{b}_T; \mu). \quad (28)$$

There is also an RG equation analogous to Eq. (21), with anomalous dimension $\gamma_D(g(\mu); \zeta_D/\mu^2)$:

$$\frac{d \ln\tilde{D}(z, \mathbf{b}_T; \mu, \zeta_D)}{d\ln\mu} = \gamma_D(g(\mu); \zeta_D/\mu^2). \quad (29)$$

For the small-$\mathbf{b}_T$ region, the collinear factorization treatment of Eq. (14), analogous to Eq. (23), gives

$$\tilde{D}_{H/f}(z, \mathbf{b}_T; \mu, \zeta_D) = \sum_j \int_z^1 \frac{d\hat{z}}{\hat{z}^{3-2\epsilon}} \tilde{C}_{j/f}(z/\hat{z}, b_T; \zeta_D, \mu, g(\mu)) d_{h/j}(\hat{z}; \mu) + \mathcal{O}((\Lambda_{\rm QCD} b_T)^a). \quad (30)$$

The analogue of Eq. (26) for the TMD FF is

$$\tilde{D}_{H/f}(z, \mathbf{b}_T; \mu, \zeta_D) = \sum_j \int_z^1 \frac{d\hat{z}}{\hat{z}^{3-2\epsilon}} \tilde{C}_{j/f}(z/\hat{z}, b_*; \mu_b^2, \mu_b, g(\mu_b)) d_{H/j}(\hat{z}, \mu_b) \times \exp\left\{\ln\frac{\sqrt{\zeta_D}}{\mu_b}\tilde{K}(b_*; \mu_b) + \int_{\mu_b}^{\mu}\frac{d\mu'}{\mu'}\left[\gamma_D(g(\mu'); 1) - \ln\frac{\sqrt{\zeta_D}}{\mu'}\gamma_K(g(\mu'))\right]\right\} \exp\left\{g_{h/j}(z, b_T) + g_K(b_T)\ln\frac{\sqrt{\zeta_D}}{\sqrt{\zeta_{D,0}}}\right\}. \quad (31)$$

As with the TMD PDF, the perturbative parts of Eq. (26) have been calculated to order α_s and are supplied for reference in the appendices. [Note the factor of $\hat{z}^{2\epsilon-3}$ that appears in the integration measure in Eq. (31) as compared to the $\hat{x}^{-1}$ factor that appears in Eq. (26); this is due to differences in normalization of the integrated PDFs and FFs.] The nonperturbative function $g_K(b_T)$ is the same in both the TMD PDF and FF. The function $g_{h/j}(z, b_T)$ describes the nonperturbative large-b_T behavior that is specific to a fragmentation function for parton j and hadron H. The momentum-space TMD FF is defined to be

$$D_{H/f}(z, z\mathbf{k}_T; \mu, \zeta_D) = \frac{1}{(2\pi)^2}\int d^2\mathbf{b}_T e^{-i\mathbf{k}_T\cdot\mathbf{b}_T} \times \tilde{D}_{H/f}(z, \mathbf{b}_T; \mu, \zeta_D). \quad (32)$$

Note that the standard momentum-space definition has $z\mathbf{k}_T$ as the transverse momentum argument rather than $\mathbf{k}_T$.

The important result of this section is that we now have expressions for the evolved TMD quark PDF and FF that can be used in Eq. (2), which in turn has a very similar structure to the generalized parton-model picture in Eq. (1).

VI. IMPLEMENTING EVOLUTION

We now discuss explicit calculations of evolved momentum-space TMDs. Given some nonperturbative input for the large-b_T behavior at some fixed scales, we can calculate the TMDs at different scales by directly calculating Eqs. (26)–(31). We will discuss the TMD PDF and FF cases separately.

A. TMD PDFs

We first analyze the TMD PDF by discussing each factor labeled in Eq. (26) separately. The first factor (the A factor) matches the TMD PDF to a collinear treatment in the small $b_T \ll 1/\Lambda_{\rm QCD}$ limit. As with standard collinear factorization, it involves a hard part, which in this case is the coefficient function $\tilde{C}_{f/j}$, and a collinear factor, which is just the standard integrated PDF. At lowest order in a calculation of the coefficient function, the A factor is simply $f(x, \mu_b)$. The first factor on the second line, the B factor, is an exponential of quantities that can all be calculated perturbatively. They are the CS kernel $\tilde{K}(b_*; \mu_b)$ at small b_T, the anomalous dimension γ_F of the TMD PDF, and the anomalous dimension γ_K of the CS kernel. The last factor, the C factor, implements the matching between the small and large b_T dependence. The function $g_{j/P}(x, b_T)$ parametrizes the nonperturbative large-b_T behavior that is intrinsic to the proton, while $g_K(b_T)$ parametrizes the nonperturbative large-$\mathbf{b}_T$ behavior of $\tilde{K}(\mathbf{b}_T; \mu)$. The function $g_{j/P}(x, b_T)$ is universal, but in principle depends on the external hadron. The function $g_K(b_T)$ is both universal and independent of the species of external hadrons. Note that,

while the description of the b_T behavior becomes nonperturbative at large b_T, there is still perturbatively calculable evolution for the TMD coming from the B factor.

For doing calculations, a choice for the numerical values of ζ_F and ζ_D in Eqs. (26)–(31) is needed. Since $\sqrt{\zeta_F\zeta_D} \approx Q^2$, we will treat the PDFs and FFs symmetrically and use $\sqrt{\zeta_F} = \sqrt{\zeta_D} = Q$. (In principle, slightly different choices may be preferred in specific applications, but this will be sufficient for now.) Also, we relabel $\sqrt{\zeta_{F,0}} = \sqrt{\zeta_{D,0}} \equiv 2Q_0$.

It is instructive to investigate the relationship between the parton-model expectation and Eq. (26). In standard collinear factorization for processes integrated over transverse momentum, the parton-model description of the *integrated* PDF is recovered by dropping all order-α_s contributions to the DGLAP evolution kernel, reproducing the Bjorken scaling property of the parton model. In collinear factorization, the parton model can be understood as the zeroth order contribution to the full pQCD factorization result. In the TMD PDF case, however, if all order-α_s or higher contributions to Eq. (26) are dropped, then the TMD PDF becomes

$$\tilde{F}_{f/P}(x, \mathbf{b}_T; \zeta_F, \mu) \to f_{j/P}(x) \exp\left\{g_{j/P}(x, b_T) + g_K(b_T) \times \ln\frac{Q}{2Q_0}\right\}. \quad (33)$$

Usually, a Gaussian model is used in a partonic description of the TMD PDF like Eq. (1). So we write $g_{j/P}(x, b_T)$ as $-g_1 b_T^2/2$ and $g_K(b_T)$ as $-g_2 b_T^2/2$. Then Eq. (33) becomes

$$f_{j/P}(x) \exp\left\{-\left[g_1 + g_2 \ln\frac{Q}{2Q_0}\right]\frac{b_T^2}{2}\right\}. \quad (34)$$

This is almost the Gaussian/parton-model form of the TMD PDF. However, there is still scale dependence coming from the coefficient of the $g_K(b_T)$ function. This difference from the collinear case is due to the fact that, while the DGLAP evolution kernels vanish when order-α_s terms are neglected, the evolution kernel in Eq. (19) is nonvanishing at zeroth order because of the nonperturbative contribution at large b_T. TMD factorization therefore differs in a significant qualitative way from collinear factorization in that the naive expectation from the parton-model picture is not exactly recovered even in a zeroth order treatment—there is still potentially large scale dependence at large b_T. This can have a large effect on the small-k_T scale dependence of the TMDs, as already noted in Refs. [39,40]. In particular, if $g_1 \ll g_2$, then it can be seen from Eq. (34) that the TMD PDF becomes extremely sensitive to Q near $Q \sim 2Q_0$ and at large b_T. In the momentum-space TMD PDF, the evolution corresponds to rapid suppression at small k_T, of order $k_T \sim 1$ GeV, with increasing Q. The effect can be observed in the small-k_T region of the curves in Fig. 1.

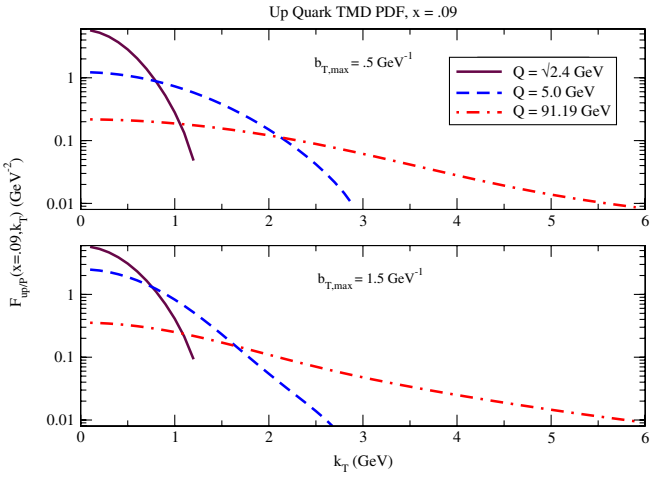

FIG. 1 (color online). The up quark TMD PDF for $Q = \sqrt{2.4}$, 5.0, and 91.19 GeV and $x = 0.09$. The upper plot shows the result of using the BLNY fit in Eq. (38) with $b_{\max} = 0.5$ GeV^{-1} while the lower panel shows the BLNY fit obtained with $b_{\max} = 1.5$ GeV^{-1}. The solid maroon, dashed blue, and red dot-dashed curves are for $Q = \sqrt{2.4}$, 5.0, and 91.19 GeV, respectively. (See online version for color.)

Once the A and B and C factors are known, it becomes straightforward to calculate the Fourier transform in Eq. (27). Of these, the A factor is the most cumbersome to deal with because it requires numerical integrals over x that involve integrated PDFs. The integrated PDFs themselves need to be imported from previous fits. In our calculations, we obtain the A factor in Eq. (26) by using the Martin-Stirling-Thorne-Watt (MSTW) PDFs [67], along with the $\overline{\text{MS}}$ coefficient functions calculated in Appendix A. To facilitate future calculations, we have made separate tables for the A factor available for each quark flavor [41]. The B factor, up to order α_s, is straightforward to calculate directly using the anomalous dimensions provided in Appendix B.

All that is then needed to obtain Eq. (27) is a model or a fit of the nonperturbative $\mathbf{b}_T$ behavior of the C factor. For our calculations, we appeal to currently available fits. In principle, fitting the nonperturbative parts, $g_{j/P}(x, b_T)$ and $g_K(b_T)$, requires knowledge of the complete $(x, \mathbf{b}_T)$ plane at different values of Q and for each flavor. There have been extensive efforts over the past several decades to determine these parameters from experiments, most commonly from fits to DY processes. Currently, the most detailed global fits use the Brock-Landry-Nadolsky-Yuan (BLNY) form for the full nonperturbative $\mathbf{b}_T$ dependence, which leads to a factor in the full cross section equal to [38]

$$\exp\left\{-\left[g_1 + g_2 \ln\frac{Q}{2Q_0} + g_1 g_3 \ln(100 x_A x_B)\right] b_T^2\right\}. \quad (35)$$

The variables x_A and x_B are the usual momentum fraction variables of the annihilating quark and antiquark. This almost gives the simple form in Eq. (34), but now there

is a term in the exponent with explicit x dependence. In the $p\bar{p}$ cross section, two C factors appear; one with a function $g_{j/P}(x, b_T)$ for the probability of finding a quark in a proton, and the other with a function $g_{\bar{j}/\bar{P}}(x, b_T)$ for finding an antiquark in an antiproton. Assuming flavor independence, the symmetric role of the PDFs in the DY factorization formula allows for an immediate identification of the C-factor contribution to the TMD PDF in Eq. (26):

$$\exp\left\{-\left[\frac{g_2}{2}\ln\frac{Q}{2Q_0}+g_1\left(\frac{1}{2}+g_3\ln(10x)\right)\right]b_T^2\right\}. \quad (36)$$

The fits of Ref. [38] found $g_1 = 0.21$ GeV^2, $g_2 = 0.68$ GeV^2, and $g_3 = -0.6$, using $Q_0 = 1.6$ GeV using data from Refs. [68–73]. However, these fits mix data for $p\bar{p}$, pp, and pCu scattering which means that it must be assumed that the nonperturbative functions $g_{j/P}(x, b_T)$, $g_{\bar{j}/P}(x, b_T)$, and $g_{j/Cu}(x, b_T)$ are similar. This is not a serious problem at large Q because then the Q behavior comes mainly from the $g_K(b_T)$ function which is independent of external hadrons. However, we also want our TMD PDF to be valid at smaller $Q \lesssim Q_0$ scales, relevant to many SIDIS experiments. Our strategy then is to match the BLNY fit to the recent scale-independent Gaussian fits by Schweitzer, Teckentrup, and Metz (STM) [32]. Using HERMES SIDIS data [74,75] for $\langle x\rangle = 0.09$, $\langle Q^2\rangle \approx 2.4$ GeV^2, and $z > 0.2$, they find

$$F_{f/P}(x, \mathbf{k}_T) = f_{f/P}(x)\frac{\exp[-k_T^2/\langle k_T^2\rangle]}{\pi\langle k_T^2\rangle} \quad (37)$$

with $\langle k_T^2\rangle = (0.38 \pm 0.06)$ GeV^2. To recover this in our fit, we modify the BLNY parametrization in Eq. (36) by rewriting it as

$$\exp\left\{-\left[\frac{g_2}{2}\ln\frac{Q}{2Q_0}+g_1\left(\frac{1}{2}+g_3\ln\left(10\frac{xx_0}{x_0+x}\right)\right)\right]b_T^2\right\}. \quad (38)$$

If $x_0 \approx 0.02$, then Eq. (38) approximately matches the STM fit for $x = 0.09$ and $Q = \sqrt{2.4}$ GeV, but reduces to the BLNY fit at larger Q and smaller x. We note that the x and $\mathbf{b}_T$ dependence does not quite factorize in these TMD fits. Indeed, the form of the $g_{j/P}(x, b_T)$ is not required by the formalism to factorize into separate x and $\mathbf{b}_T$ dependence.

We now have a fit that includes the scale dependence of the QCD evolution in Eq. (26), and whose b_T dependence matches two previously performed fits for different regions of kinematics. For illustration, we have plotted in Fig. 1 the TMD PDF of the up-quark for the small, medium, and large values of $Q = \sqrt{2.4}$, 5, and 91.19 GeV and with $x = 0.09$. We have made the plot run over a range from $k_T = 0$ to 6 GeV, typical for studies of TMD functions. [Recall, however, that without the Y term of Eq. (2) the TMD PDF by itself only has a simple interpretation for $k_T \ll Q$.] Comparing the curves, it is clear that the evolution in Q is a large effect, leading to more than an order of magnitude of suppression at small k_T, and a broad tail at larger k_T. Numerical computations that produce plots like Fig. 1 are available at Ref. [41]. The large b_T cutoff, $b_{\max}$, should be small enough to exclude the nonperturbative large b_T regime from the perturbative part of the TMD PDF, but it is otherwise arbitrary. In fits, different choices of $b_{\max}$ can lead to very different values for the nonperturbative parameters because changing the size of $b_{\max}$ effectively reshuffles contributions to the TMD PDF between the different factors in Eq. (26). It turns out that the $b_{\max} = 0.5$ GeV^{-1} value from the BLNY fit is rather small. In other words, this choice of $b_{\max}$ restricts the perturbative part of the calculation to a range in b_T that is significantly smaller than the range where perturbative methods are still reasonable. The analysis in Ref. [76] has found that $b_{\max} = 1.5$ GeV^{-1} is preferred, and the parameters for the BLNY fit in Eq. (35) become $g_1 = 0.201$ GeV^2, $g_2 = 0.184$ GeV^2, and $g_3 = -0.129$. By using the newer parameters from Ref. [76], we can again construct a TMD PDF parametrization from the BLNY form that matches the STM fit at small Q by using Eq. (38). With the newer parameters we find that $x_0 = 0.009$ is needed to fit to the STM parametrization at small k_T.

One reason that we prefer the smaller $b_{\max}$ for the present paper is that our present analysis includes only the order-α_s contributions to the perturbatively calculable parts, so it is important that higher order contributions are small. In practice, higher order contributions can have a large effect, especially at small and intermediate k_T. We estimate the size of the theoretical error in our analysis by redoing the calculation for the parametrization with the larger value of $b_{\max} = 1.5$ GeV^{-1}, and using the parameters of Ref. [76]. The result is the lower panel in Fig. 1. By comparing the upper and lower plots, it can be seen that the curves differ by a maximum of about a factor of 2 for the large Q curve. (By running the calculation for different values of x, we have verified that this is generally true for x between about 0.01 and 0.2.) The largest difference is for the $Q = 5$ GeV curves. This is because for $Q = 5$ GeV evolution effects become significant, but the different values of x_0 needed for the curves to match at Q_0 lead to a significant difference in k_T dependence.

In the future, it will be possible to decrease the theoretical uncertainty in the TMD PDF parametrization by including higher orders in the perturbative parts of the calculation, and by using improved fits based on newly available data.

It is also instructive to investigate the effect of the separate A, B, and C factors in Eq. (26). In Fig. 2, we have again plotted the TMD PDF for $Q = 91.19$ GeV. In addition, we show the effect of replacing the A factor by simply the lowest order, unevolving result, $f(x, \mu_{b_{\max}})$ (blue dashed curve), and the effect of replacing the B factor by one (maroon dash-dotted curve). (The color version is

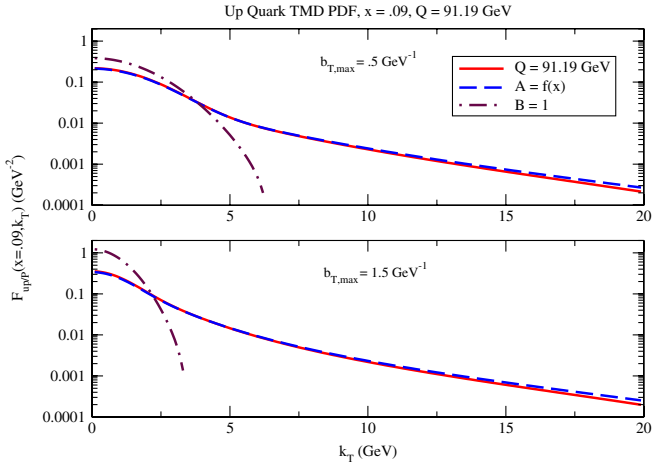

FIG. 2 (color online). Comparing the shape of the TMD PDF within various approximations. The solid red curves are the same as the $Q = 91.19$ GeV curves in Fig. 1. The dashed blue curve is the result of setting the A factor in Eq. (26) equal to $f(x, \mu_b)$, and the dash-dotted maroon curve is obtained by setting the B factor in Eq. (26) equal to 1. (See online version for color.)

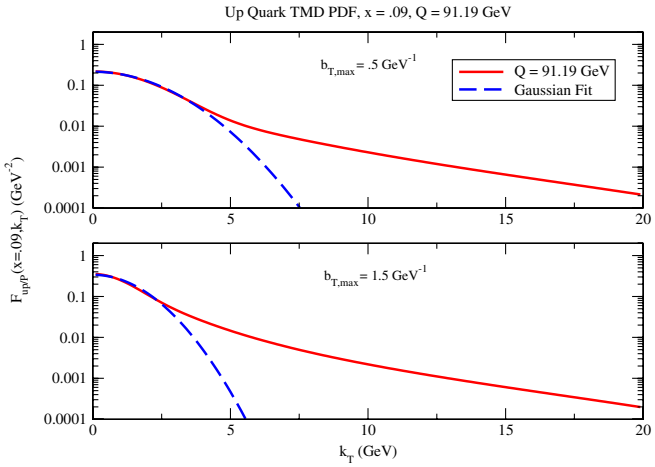

FIG. 3 (color online). Comparison of the TMD PDF at $Q = 91.19$ GeV with a Gaussian fit for the two different values of $b_{\max} = 0.5, 1.5\ \mathrm{GeV}^{-1}$. (See online version for color.)

online.) The dashed curves show that simply using $f(x, \mu_{b_{\max}})$ instead of the full A factor is typically a very good approximation in the small-k_T limit of the TMD PDF. This significantly simplifies the calculation of the TMD PDF in cases where the very small-k_T region is the main contribution of interest. (However, it should be reemphasized that the full A factor is needed for a complete description of the cross section over all q_T up to order Q.) Neglecting the B factor introduces a substantial error at small k_T and completely removes the large-k_T tail. We have compared the calculations for the two different $b_{\max}$ values, 0.5 GeV^{-1} and 1.5 GeV^{-1}, in the upper and lower plots. As could be expected, the effect of setting $B = 1$ is substantially larger in the $b_{\max} = 1.5\ \mathrm{GeV}^{-1}$ case where the role of higher orders is more important.

It is common in TMD studies to use Gaussian parametrizations like Eq. (37). An attractive feature of such an approach is that the TMD has a simple and well-defined integral over all k_T, and the standard integrated PDF is obtained simply by integrating the TMD PDF. Moreover, the Gaussian form makes the calculation of weighted structure functions simple. Therefore, it is useful to investigate how well a Gaussian form describes the shape of the TMD, and over what range of transverse momentum. (However, we recall that the actual relationship between integrated and TMD PDFs is more complicated, as already evidenced by the broad tail in Fig. 2.) To give an example of such a comparison, and to study the effect of the tail in fits of the TMD PDF at large Q, we have replotted the $Q = 91.19$ GeV curves from Fig. 1 in Fig. 3, but now we include Gaussian fits. From the plots it can be seen that at large-Q the Gaussian shape continues to do a reasonable job of describing the very small k_T behavior (less than a few GeV), but since it completely neglects the tail at large k_T tail it underestimates the size of the typical k_T.

To investigate the role of the tail, we calculated the integral of the TMD PDF over k_T, weighted by k_T^2,

$$\bar{k}_T^2 = \int d^2\mathbf{k}_T k_T^2 F(x, \mathbf{k}_T), \tag{39}$$

and we compared the result of using the Gaussian fit with the result obtained by numerically integrating the original $Q = 91.19$ GeV curve (the solid curve in Fig. 3). For the original curve, Eq. (39) is quite ill defined because of the large-k_T tail. In addition, the contribution from very large k_T is outside the region where a TMD-factorization description alone is valid, and the Y term becomes important. Nevertheless, it is possible to get a sense of the effect of the tail on typical values of k_T by integrating up to a cutoff that is large, but still significantly less than Q. For the TMD PDFs in Fig. 3, we choose an upper cutoff of 20 GeV. For the Gaussian fit, we find $\sqrt{\bar{k}_T^2} = 6$ GeV for $b_{\max} = 0.5\ \mathrm{GeV}^{-1}$ and $\sqrt{\bar{k}_T^2} = 4$ GeV for $b_{\max} = 1.5\ \mathrm{GeV}^{-1}$. (The difference is due to the slightly different ranges in k_T where a Gaussian is a good fit.) For the original curve, with the upper cutoff on k_T of 20 GeV, we find $\sqrt{\bar{k}_T^2} = 15$ GeV for both $b_{\max} = 0.5\ \mathrm{GeV}^{-1}$ and $b_{\max} = 1.5\ \mathrm{GeV}^{-1}$. Hence, for both values of $b_{\max}$, the tail leads to at least a factor of 2 increase in the typical k_T.

B. TMD FFs

The nonperturbative input for the FFs is much less constrained by existing analyses. However, the function $g_K(b_T)$ in Eq. (26) for the TMD PDF is the same function that appears in Eq. (31) for the TMD FF. Therefore, given a fit for the TMD FF at a particular scale, one can use the same $g_K(b_T)$, along with the anomalous dimensions and

coefficient functions calculated in Appendices A and B, to estimate the evolution to different scales. For the starting scale, we again appeal to the fit of Ref. [32] which uses a Gaussian form,

$$D_{H/f}(z, \mathbf{K_T}) = d_{H/f}(z)\frac{\exp[-K_T^2/\langle K_T^2\rangle]}{\pi\langle K_T^2\rangle}, \qquad (40)$$

where K_T is the hadron transverse momentum in the photon rest frame. Again fitting the HERMES data, for SIDIS in the kinematical range, $\langle x\rangle = 0.09$, $\langle Q^2\rangle \approx 2.4$ GeV^2, and $z > 0.2$, they find that $\langle K_T^2\rangle = (0.16 \pm 0.01)$ GeV^2. One can write the transverse components of the photon-frame hadron momentum $\mathbf{K}_T$ in terms of the transverse components of the hadron-frame parton momentum $\mathbf{k}_T$ as $\mathbf{K}_T = -z\mathbf{k}_T$. The analogue of Eq. (34) for the FF has an extra $1/z^2$ so that when all order α_s corrections are dropped the FF reads

$$\tilde{D}_{H/f}(z, b_T; \zeta_F, \mu) \to \frac{1}{z^2} d_{H/f}(z) \times \exp\left\{-[g_1' + g_2 z^2 \ln\frac{Q}{2Q_0}]\frac{b_T^2}{2z^2}\right\}. \qquad (41)$$

Equating this to the inverse Fourier transform of Eq. (40), we identify the factor in brackets as

$$g_1' + g_2 z^2 \ln\frac{\sqrt{2.4\ \text{GeV}}}{2Q_0} \approx \frac{\langle K_T^2\rangle}{2} \approx 0.08\ \text{GeV}.$$

From this relation we can extract a value for g_1'. The factor multiplying $-b_T^2$ in Eq. (41) can then be identified with the nonperturbative exponential factor in Eq. (31). Using Refs. [77–80] for the integrated FFs, we can then calculate the TMD FF using Eq. (31). We have repeated the analysis of the TMD PDF for a TMD FF of a charged pion fragmenting from an up quark. Figure 4 shows the TMD FF for different energy scales, $Q = \sqrt{2.4}$, 5, and 91.19 GeV. By comparing different energy scales, one can immediately see the effect of including perturbative evolution in the definitions of the TMD FFs from the high k_T tails the TMD FFs acquire. We have also repeated the analysis of evaluating the TMD FF for different values of $b_{\max} = 0.5$ and 1.5 GeV^{-1} and we find a similar error estimate as in the case of the TMD PDF. The comparison is shown again in Fig. 4. Note that in Fig. 4 we have plotted the TMD FF as a function of the *hadron* transverse momentum K_T rather than parton transverse momentum k_T.

We also investigated how well a Gaussian function fits the perturbatively evolved TMD FF. As with the TMD PDF, the Gaussian fit does not adequately capture the effects of perturbative evolution for the TMD FF. The contribution of the k_T tail is smaller in the case of the TMD FF. This can be understood by comparing the k_T dependence of a TMD PDF with a TMD FF. The TMD FF is less broad in k_T than a TMD PDF and therefore drops

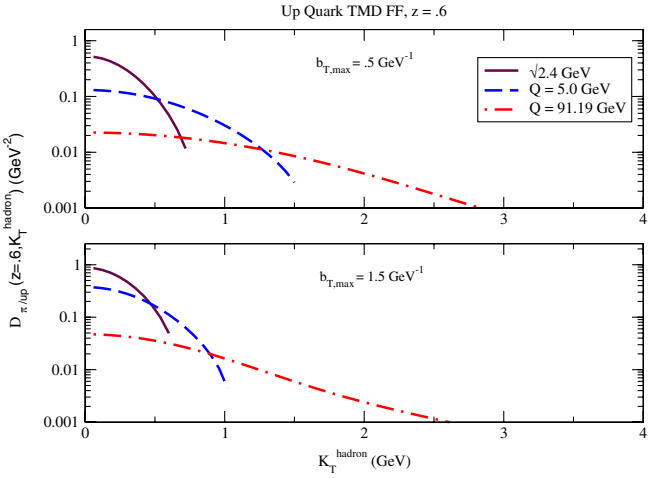

FIG. 4 (color online). TMD FF for charged pions from a hadronizing up quark. The upper plot is for $g_2 = 0.68$ GeV^2 and the lower plot is for $g_2 = 0.184$ GeV^2. In each case, TMD FF matches to the STM fit at $Q = \sqrt{2.4}$ GeV. (See online version for color.)

faster with a smaller k_T tail. To quantify this we have once more calculated a typical k_T using Eq. (39) both for the Gaussian fit and the actual TMD FF. For $b_{\max} = 0.5$ GeV^{-1} we find that for the Gaussian fit $\sqrt{\bar{k}_T^2} = 1.74$ GeV while for the actual TMD FF $\sqrt{\bar{k}_T^2} = 2.15$ GeV which gives a relative difference of 23.5%. For the case of $b_{\max} = 1.5$ GeV^{-1} the values are $\sqrt{\bar{k}_T^2} = 1.06$ GeV for the Gaussian fit and $\sqrt{\bar{k}_T^2} = 1.85$ GeV for the actual TMD FF with a larger relative difference of 73.5%.

VII. DISCUSSION AND CONCLUSIONS

Factorization theorems provide the bridge between abstract field theoretical concepts and phenomenology, and are responsible for giving pQCD its great predictive power. The parton distribution and fragmentation functions, which arise naturally from the factorization derivations, play a central role in relating formal pQCD to parton-model concepts. A precise understanding of the definitions, evolution, and universality properties of these correlation functions is what enables calculations in pQCD to make accurate first principles predictions.

While the standard formalism of collinear factorization has proven extremely useful for sufficiently inclusive processes, the more sophisticated formalism of TMD factorization is needed for processes in which the intrinsic transverse momentum of the partons becomes important. As has already been widely discussed, there are a number of technical and conceptual subtleties involved in arriving at good definitions for the TMDs that are consistent with factorization. These issues include the need to regulate and deal with rapidity divergences and achieve a cancellation

of spurious Wilson line self-energies. The subtleties involved in defining TMDs have largely been clarified and resolved in Ref. [25], which provides definitions that are consistent with the requirements of factorization, and demonstrates the relationship with the usual CSS formalism.

While considerable effort has been devoted to implementing CSS evolution in unpolarized scattering, the resulting parametrizations are often not framed in the language of TMD PDFs. By contrast, for polarization dependent TMDs, there has been very little work done in implementing evolution in the parametrization of experimental data. Up to this point, these functions have only been probed over a very narrow range of scales so that evolution has not been a major issue. However, for future progress in understanding the role of quark and gluon degrees of freedom in hadronic structure, it will be important to remedy this situation. Ideally, there should be collections of tabulated fits to the TMDs that incorporate evolution, and which can be directly related to the field-theoretic definitions of the correlation functions, analogous to what has already existed for some time in collinear factorization.

We have started this process by recasting previously performed fits [32,37,38] of unpolarized TMD PDFs and TMD FFs in terms of the TMD definitions of Ref. [25]. This provides a much clearer connection between the formalism of evolution and generalized parton model approaches, and provides practical TMD parametrizations that can be used directly in TMD calculations. We have also completed the derivation of the lowest order anomalous dimensions and coefficient functions for the TMD PDF. At our website [41], we have supplied tables and interpolation routines for the parts of the quark TMD PDFs and FFs that can be described using collinear factorization [the "A factors" in Eqs. (26) and (31)] for each flavor of quark, as well as sample calculations that give plots like Fig. 1.

We have confirmed the important observation that evolution has a strong quantitative effect on the TMDs and therefore should be included in future phenomenological applications of TMD factorization, particularly given the range of energy scales that are set to be probed in the future. Another reason to have reliable fits of TMDs, including evolution, is that it opens the possibility to identify instances of factorization breaking effects of the type discussed in Refs. [45–48]. Recognizing factorization breaking effects will be an important next step in expanding our understanding of pQCD phenomenology. Even in unpolarized scattering, there is a possibility to use parametrizations like those presented in this paper to test the factorization hypothesis. Recent RHIC data [57,58], for example, may be useful for such an analysis.

Nevertheless, much work remains to be done. The theoretical uncertainty in the TMD fits can be reduced by including higher orders in the calculations of the anomalous dimensions, the K kernel, and the collinear coefficient functions. Moreover, as new data from experiments like those taking place at the LHC, RHIC, JLab, and a possible electron-ion collider are made available and analyzed, it will be possible to obtain improved fits. Already, there are data from ATLAS [81] which can potentially help to improve the quality of fits for the unpolarized TMDs. TMD effects can also be studied in an e^+e^- collider as recently discussed in Ref. [40]. A number of theoretical issues with the evolution formalism itself also remain unsettled. For instance, the precise form of the matching function for between perturbative and nonperturbative transverse momentum regimes in Eq. (24) is somewhat arbitrary and better prescriptions may be possible. Along similar lines, a truly optimal choice of $b_{\max}$ may be different from the values we have used here. One possibility may be to formulate the evolution directly in momentum space.

One of the most important next steps is to extend the analysis presented in this paper to the Sivers and Boer-Mulders functions, which are needed for clarifying the spin structure of hadrons. Efforts to address polarization dependent situations can utilize existing fixed-scale fits (such as [27–32,51]). In such cases, a careful treatment of the matching between large and small transverse momenta will also be important [82]. Furthermore, it will be important to establish the relationship be evolved TMDs and the evolution of weighted functions such as those treated in Ref. [43].

Fits of the gluon TMD PDF that include CSS evolution will be also be needed, especially in tests of factorization. See [83,84] for recent work related to evolution and gluon resummation in the context of gluon PDFs. In addition, recent calculations in Ref. [85] have shown how to probe linearly polarized gluons in heavy quark production, and the universality properties of the gluon TMD PDF have been clarified in Ref. [86]. For processes that probe the gluon TMDs, some important details of the TMD-factorization theorems have yet to be completely understood. The issue of so-called "superleading regions" in the factorization theorems that use the gluon distribution [87] still needs to be clarified in the TMD case. Furthermore, for processes that involve several final state hadrons, such as $e + p \to H_1 + H_2 + X$, the separation of the soft factor into universal square root factors as in the definitions in Eqs. (12)–(14) is not straightforward. Following a naive analysis like in Sec. IV C seems to suggest that extra soft factors are needed, and that a more complicated factorization structure is required.

These are all issues we intend to pursue in a continuation of the TMD project.

ACKNOWLEDGMENTS

We especially thank J. Collins for many useful discussions regarding his book. Helpful comments were also

provided by C. Aidala, D. Boer, M. Buffing, A. Metz, and P. Mulders. We thank P. Nadolsky for discussions of the BLNY fits, and G. Watt for help in implementing the MSTW parton distribution functions. Support was provided by the research program of the "Stichting voor Fundamenteel Onderzoek der Materie (FOM)", which is financially supported by the "Nederlandse Organisatie voor Wetenschappelijk Onderzoek (NWO)". M. Aybat also acknowledges support from the FP7 EU-program HadronPhysics2 (Contract No. 2866403). All Feynman graphs were made using JAXODRAW [88].

APPENDIX A: COEFFICIENT FUNCTIONS

In this Appendix, we present the steps for calculating the collinear coefficient functions [the $\tilde{C}_{f/j}(x/\hat{x}, b_*; \mu_b^2, \mu_b, g(\mu_b))$ functions in the A factor of Eq. (26)]. We first briefly review the steps, presented in Ref. [25], for the case of the TMD FFs. Then we explain the extension to the analogous case for the TMD PDFs.

In perturbation theory, the FF in Eq. (13) itself obeys a collinear factorization theorem [3], valid for small $\mathbf{b}_T$. The collinear part is just the standard integrated FF. Writing the factorization as $\tilde{D} = d \otimes C$, we have to first order

$$\tilde{D}^{[1]} = d^{[0]} \otimes \tilde{C}^{[1]} + d^{[1]} \otimes \tilde{C}^{[0]}. \tag{A1}$$

The superscripts label the order in perturbation theory. Using $d^{[0]}_{j/j'}(z) = \delta_{jj'}\delta(z-1)$ for the lowest order integrated FF, one finds

$$\tilde{C}^{[1]}_{j/f}(z, \mathbf{b}_T) = \tilde{D}^{[1]}_{j/f}(z, \mathbf{b}_T) - \frac{d^{[1]}_{j/f}(z)}{z^{2-2\epsilon}}, \tag{A2}$$

for the first order FF coefficient function. To get the collinear coefficient function, all that is needed then is to calculate the first order expression for the unintegrated FF $\tilde{D}^{[1]}_{j/f}(z, \mathbf{b}_T)$ and for the integrated case $d_{j/f}(z)$. Since $\tilde{C}^{[1]}_{j/f}(z, \mathbf{b}_T)$ is independent of the species of external hadron, the calculation can be done for the special case of a quark hadronizing to a gluon.

The order $\mathcal{O}(g^2)$ diagram is shown in Fig. 5. There is no leading contribution from the soft region and, hence, no need to subtract soft-factor contributions. Calculating the first order TMD FF gives

$$\begin{aligned}\tilde{D}^{[1]}_{g/q}(z, \mathbf{b}_T) &= \frac{g^2\mu^{2\epsilon}C_F}{(2\pi)^{4-2\epsilon}z}\int dk^- d^{2-2\epsilon}\mathbf{k}_T e^{i\mathbf{k}_T\cdot\mathbf{b}_T} \\ &\quad\times 2\pi\delta((k-p)^2)\frac{1}{4}\frac{\mathrm{Tr}\sum_j \gamma^+ \not{k}\gamma^j(\not{k}-\not{p})\gamma^j\not{k}}{(k^2)^2} \\ &= \frac{g^2(4\pi^2\mu^2)^\epsilon C_F}{8\pi^3}\int\frac{d^{2-2\epsilon}\mathbf{k}_T e^{i\mathbf{k}_T\cdot\mathbf{b}_T}}{k_T^2} \\ &\quad\times\left[\frac{1+(1-z)^2-\epsilon z^2}{z^3}\right].\end{aligned} \tag{A3}$$

The corresponding integrated FF is calculated in nearly the same way, except that $\mathbf{b}_T$ is set to zero and the $1/z$ factor in the definition (13) is changed to $z^{2\epsilon-1}$ in the integrated case. Also, an $\overline{\mathrm{MS}}$ counterterm is needed to remove the resulting UV divergence. The result is

$$\begin{aligned}d^{[1]}_{g/q}(z) &= \frac{g^2(4\pi^2\mu^2)^\epsilon C_F}{8\pi^3}\int\frac{d^{2-2\epsilon}\mathbf{k}_T}{k_T^2}\left[\frac{1+(1-z)^2-\epsilon z^2}{z^{1+2\epsilon}}\right] \\ &\quad - \frac{g^2 C_F(4\pi)^\epsilon}{8\pi^2\Gamma(1-\epsilon)\epsilon}\left[\frac{1+(1-z)^2}{z}\right].\end{aligned} \tag{A4}$$

Performing the k_T integrals and putting all the terms together in Eq. (A2) gives the collinear coefficient function,

$$\begin{aligned}&\tilde{C}_{g/j'}(z, \mathbf{b}_T; \mu; \zeta_D/\mu^2) \\ &= \frac{\alpha_s C_F}{2\pi z^3}\left(2[1+(1-z)^2]\left[\ln\left(\frac{2z}{b_T\mu}\right)-\gamma_E\right]+z^2\right) \\ &\quad + \mathcal{O}(\alpha_s^2).\end{aligned} \tag{A5}$$

For the TMD FF of a quark hadronizing to a quark, the diagrams are shown in Fig. 6, along with the soft subtraction factors in Fig. 7 that are needed according to the definition in Eq. (8). Apart from the need to include soft-factor contributions, the steps are analogous to those that led to Eq. (A5) The integrated FF is found again using Fig. 6 along with $\overline{\mathrm{MS}}$ counterterms. The result is

$$\begin{aligned}&\tilde{C}_{j/j'}(z, \mathbf{b}_T; \mu; \zeta_D/\mu^2) \\ &= \delta_{j'j}\delta(1-z) + \delta_{j'j}\frac{\alpha_s C_F}{2\pi}\left\{2\left[\ln\left(\frac{2z}{\mu b_T}\right)-\gamma_E\right]\right. \\ &\quad\times\left[\left(\frac{2}{1-z}\right)_+ + \frac{1}{z^2}+\frac{1}{z}\right] + \frac{1}{z^2} - \frac{1}{z} + \delta(1-z) \\ &\quad\times\left[-\frac{1}{2}[\ln(b_T^2\mu^2) - 2(\ln 2 - \gamma_E)]^2 - [\ln(b_T^2\mu^2)\right. \\ &\quad\left.\left.\left. - 2(\ln 2 - \gamma_E)\right]\ln\left(\frac{\zeta_D}{\mu^2}\right)\right]\right\} + \mathcal{O}(\alpha_s^2).\end{aligned} \tag{A6}$$

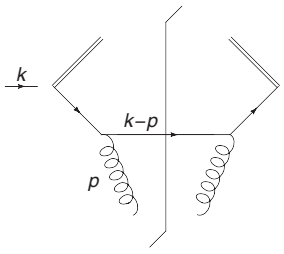

FIG. 5. One-loop diagram used contributing to the TMD FF and the integrated FF of a quark fragmenting to a gluon.

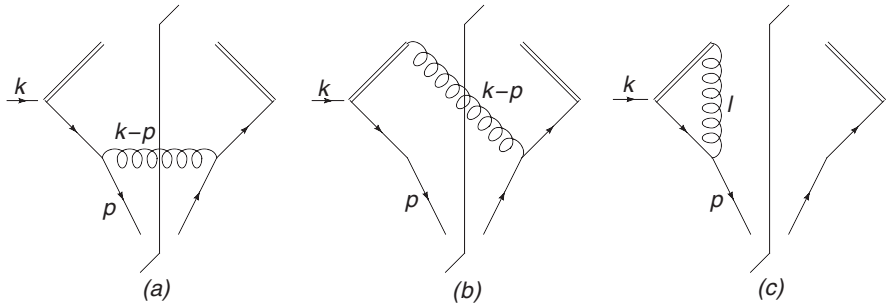

FIG. 6. One-loop diagrams contributing to the TMD FF and the integrated FF of a quark fragmenting into a quark.

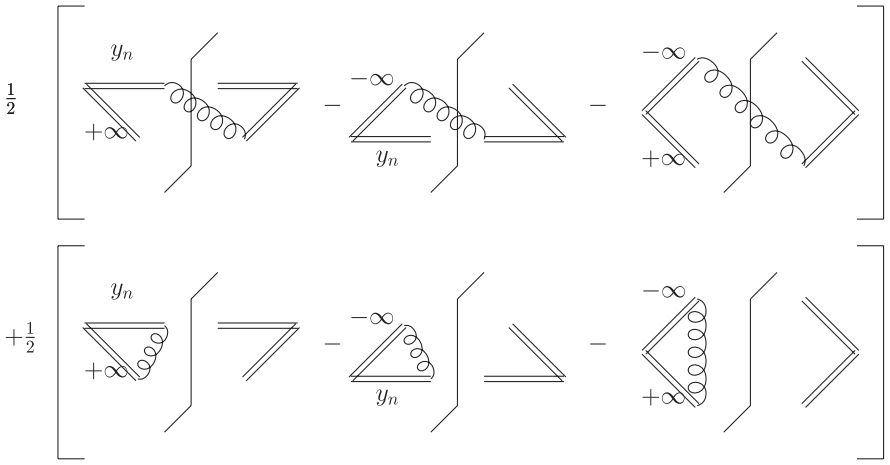

FIG. 7. One-loop diagrams for the soft-factor contributions of Eq. (31). Hermitian conjugate graphs are also needed but are not shown.

Again, the details for the above FF calculation can be found in Ref. [25].

The steps for calculating the order-$\mathcal{O}(g^2)$ contributions to the collinear coefficient functions for the TMD PDFs are analogous to the steps used in the TMD FF case, with some minor changes. We provide them here, presented for the first time in the context of TMDs. The results should be equivalent to calculations already done in the CSS formalism, up to possible changes in scheme. For the TMD PDF, the analogue of Eq. (A2) is

$$\tilde{C}^{[1]}_{j/f}(x,\mathbf{b}_T) = \tilde{F}^{[1]}_{j/f}(x,\mathbf{b}_T) - f^{[1]}_{j/f}(x). \tag{A7}$$

The difference in factors of longitudinal momentum fraction in the second term comes from the different normalization in Eq. (30) as compared with (23). Again, we may perform the calculation for on-shell external partons. Using the diagram in Fig. 8, for the TMD PDF of a quark inside a gluon one has

$$\begin{aligned}
&\tilde{F}^{[1]}_{q/g}(x,\mathbf{b}_T) \\
&= -\frac{T_f g^2 \mu^{2\epsilon}}{(2\pi)^{4-2\epsilon}(1-\epsilon)} \int dk^- d^{2-2\epsilon}\mathbf{k}_T e^{-i\mathbf{k}_T\cdot\mathbf{b}_T} 2\pi\delta((p-k)^2) \\
&\quad \times \frac{1}{4}\frac{\sum_{\text{pol}} \text{Tr}(\gamma^+ k \not{\epsilon}_p (\not{k}-\not{p})\not{\epsilon}^*_p k)}{(k^2)^2} \\
&= \frac{g^2(4\pi\mu^2)^\epsilon T_f}{8\pi^2\Gamma(1-\epsilon)} \int_0^\infty \frac{d^{2-2\epsilon}\mathbf{k}_T}{k_T^2} e^{-i\mathbf{k}_T\cdot\mathbf{b}_T}\left[1 - \frac{2x(1-x)}{1-\epsilon}\right],
\end{aligned} \tag{A8}$$

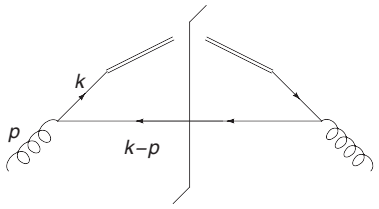

FIG. 8. One-loop diagram contributing to the TMD PDF and the integrated PDF for a quark inside a gluon.

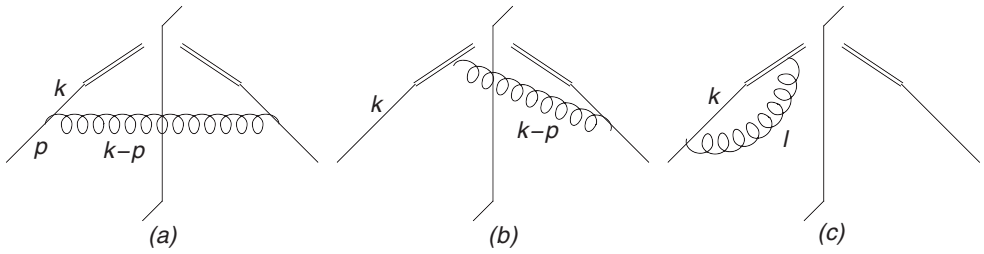

FIG. 9. One-loop diagrams contributing to the TMD PDF and the integrated PDF of a quark inside a quark. Hermitian conjugate graphs are also needed but are not shown.

where ϵ_p^μ is the polarization vector for the initial state gluon and we sum and average over all possible polarizations. The integrated PDF is found again by setting $\mathbf{b}_T = 0$ in the above equation and adding the appropriate $\overline{\text{MS}}$ counterterm for the resulting UV divergence. This gives

$$f^{[1]}_{q/g}(x) = \frac{g^2(4\pi\mu^2)^\epsilon T_f}{8\pi^2\Gamma(1-\epsilon)}\int_0^\infty dk_T^2 \frac{k_T^{-2\epsilon}}{k_T^2}\left[1 - \frac{2x(1-x)}{1-\epsilon}\right] - \frac{g^2(4\pi\mu^2)^\epsilon T_f}{8\pi^2\Gamma(1-\epsilon)\epsilon}[1-2x(1-x)]. \tag{A9}$$

Using Eqs. (A7)–(A9) and evaluating the k_T integrals, gives the TMD PDF collinear coefficient function for finding a quark of flavor j' in a gluon at order α_s,

$$\tilde{C}_{j'/g}(x, \mathbf{b}_T; \mu; \zeta_F/\mu^2) = \frac{\alpha_s T_f}{2\pi}\left\{2[1-2x(1-x)]\left[\ln\left(\frac{2}{b_T\mu}\right) - \gamma_E\right] + 2x(1-x)\right\} + \mathcal{O}(\alpha_s^2). \tag{A10}$$

Finally using diagrams in Fig. 9 together with the soft subtraction terms in Fig. 7 for the TMD PDF for finding a quark of flavor j' in a quark of flavor j and again the diagrams in Fig. 9 together with the $\overline{\text{MS}}$ UV counterterms for the integrated quark PDF, we find to order α_s,

$$\begin{aligned}\tilde{C}_{j'/j}(x, \mathbf{b}_T; \mu; \zeta_F/\mu^2) &= \delta_{j'j}\delta(1-x) + \delta_{j'j}\frac{\alpha_s C_F}{2\pi}\left\{2\left[\ln\left(\frac{2}{\mu b_T}\right) - \gamma_E\right]\right. \\ &\times\left[\left(\frac{2}{1-x}\right)_+ - 1 - x\right] + 1 - x + \delta(1-x) \\ &\times\left[-\frac{1}{2}[\ln(b_T^2\mu^2) - 2(\ln 2 - \gamma_E)]^2 - [\ln(b_T^2\mu^2) \right. \\ &\left.\left. - 2(\ln 2 - \gamma_E)]\ln\left(\frac{\zeta_F}{\mu^2}\right)\right]\right\} + \mathcal{O}(\alpha_s^2).\end{aligned} \tag{A11}$$

APPENDIX B: ANOMALOUS DIMENSIONS

All calculations of anomalous dimensions defined in Eqs. (21), (21), and (29) use dimensional regularization with the $\overline{\text{MS}}$ scheme. The anomalous dimension of the quark TMD PDF up to order α_s is

$$\gamma_F(\mu; \zeta_F/\mu^2) = \alpha_s\frac{C_F}{\pi}\left(\frac{3}{2} - \ln\left(\frac{\zeta_F}{\mu^2}\right)\right) + \mathcal{O}(\alpha_s^2). \tag{B1}$$

At order α_s, the quark TMD FF anomalous dimension is the same as for the TMD PDF. We note that these results are consistent with what is found in, e.g., Ref. [61] using different methods.

The CS kernel, in Eq. (18), up to order α_s in $\mathbf{b}_T$ space is

$$\tilde{K}(\mu, b_T) = -\frac{\alpha_s C_F}{\pi}[\ln(\mu^2 b_T^2) - \ln 4 + 2\gamma_E] + \mathcal{O}(\alpha_s^2). \tag{B2}$$

The anomalous dimension of $\tilde{K}$ [see Eq. (20)] is up to order α_s,

$$\gamma_K(\mu) = 2\frac{\alpha_s C_F}{\pi} + \mathcal{O}(\alpha_s^2). \tag{B3}$$

[1] J. C. Collins, D. E. Soper, and G. F. Sterman, Adv. Ser. Dir. High Energy Phys. **5**, 1 (1988).
[2] V. Barone, F. Bradamante, and A. Martin, Prog. Part. Nucl. Phys. **65**, 267 (2010).
[3] J. C. Collins and D. E. Soper, Nucl. Phys. **B194**, 445 (1982).
[4] J. C. Collins and D. E. Soper, Nucl. Phys. **B193**, 381 (1981); **B213**, 545(E) (1983).

[5] J. C. Collins, D. E. Soper, and G. Sterman, Nucl. Phys. **B250**, 199 (1985).
[6] C. T. H. Davies, B. R. Webber, and W. J. Stirling, Nucl. Phys. **B256**, 413 (1985).
[7] C. Balazs and C. P. Yuan, Phys. Rev. D **56**, 5558 (1997).
[8] E. L. Berger and J. w. Qiu, Phys. Rev. D **67**, 034026 (2003).
[9] E. L. Berger and J. w. Qiu, Phys. Rev. Lett. **91**, 222003 (2003).
[10] G. Bozzi, S. Catani, D. de Florian, and M. Grazzini, Nucl. Phys. **B737**, 73 (2006).
[11] R. Meng, F. I. Olness, and D. E. Soper, Phys. Rev. D **54**, 1919 (1996).
[12] P. M. Nadolsky, D. R. Stump, and C. P. Yuan, Phys. Rev. D **61**, 014003 (1999); **64**, 059903(E) (2001).
[13] X. d. Ji, J. p. Ma, and F. Yuan, Phys. Rev. D **71**, 034005 (2005).
[14] X. d. Ji, J. P. Ma, and F. Yuan, Phys. Lett. B **597**, 299 (2004).
[15] J. C. Collins and F. Hautmann, Phys. Lett. B **472**, 129 (2000).
[16] J. C. Collins and F. Hautmann, J. High Energy Phys. 03 (2001) 016.
[17] A. A. Henneman, D. Boer, and P. J. Mulders, Nucl. Phys. **B620**, 331 (2002).
[18] A. V. Belitsky, X. Ji, and F. Yuan, Nucl. Phys. **B656**, 165 (2003).
[19] D. Boer, P. J. Mulders, and F. Pijlman, Nucl. Phys. **B667**, 201 (2003).
[20] J. C. Collins, Acta Phys. Pol. B **34**, 3103 (2003).
[21] F. Hautmann and D. E. Soper, Phys. Rev. D **75**, 074020 (2007).
[22] J. C. Collins, T. C. Rogers, and A. M. Stasto, Phys. Rev. D **77**, 085009 (2008).
[23] I. O. Cherednikov and N. G. Stefanis, Phys. Rev. D **77**, 094001 (2008); I. O. Cherednikov and N. G. Stefanis, Phys. Rev. D **80**, 054008 (2009); I. O. Cherednikov, A. I. Karanikas, and N. G. Stefanis, Nucl. Phys. **B840**, 379 (2010).
[24] J. Collins, Proc. Sci., C2008 (2008) 028.
[25] J. C. Collins, *Foundations of Perturbative QCD* (Cambridge University Press, Cambridge, 2011).
[26] J. C. Collins, at the 2010 TMD Workshop, Trento, Italy [http://www.pv.infn.it/ bacchett/TMDprogram.htm].
[27] M. Anselmino, M. Boglione, U. D'Alesio, E. Leader, and F. Murgia, Phys. Rev. D **70**, 074025 (2004).
[28] M. Anselmino, M. Boglione, U. D'Alesio, E. Leader, S. Melis, and F. Murgia, Phys. Rev. D **73**, 014020 (2006).
[29] M. Anselmino, M. Boglione, U. D'Alesio, A. Kotzinian, F. Murgia, A. Prokudin, and C. Turk, Phys. Rev. D **75**, 054032 (2007).
[30] M. Anselmino *et al.*, Eur. Phys. J. A **39**, 89 (2008).
[31] M. Anselmino, M. Boglione, U. D'Alesio, S. Melis, F. Murgia, and A. Prokudin, Phys. Rev. D **79**, 054010 (2009).
[32] P. Schweitzer, T. Teckentrup, and A. Metz, Phys. Rev. D **81**, 094019 (2010).
[33] U. D'Alesio and F. Murgia, Prog. Part. Nucl. Phys. **61**, 394 (2008).
[34] H. Avakian, A. V. Efremov, P. Schweitzer, O. V. Teryaev, F. Yuan, and P. Zavada, Mod. Phys. Lett. A **24**, 2995 (2009).
[35] S. J. Brodsky, D. S. Hwang, and I. Schmidt, Phys. Lett. B **530**, 99 (2002).
[36] S. J. Brodsky, D. S. Hwang, and I. Schmidt, Nucl. Phys. **B642**, 344 (2002).
[37] G. A. Ladinsky and C. P. Yuan, Phys. Rev. D **50**, R4239 (1994).
[38] F. Landry, R. Brock, P. M. Nadolsky, and C. P. Yuan, Phys. Rev. D **67**, 073016 (2003).
[39] D. Boer, Nucl. Phys. **B603**, 195 (2001).
[40] D. Boer, Nucl. Phys. **B806**, 23 (2009).
[41] http://projects.hepforge.org/tmd/.
[42] J. w. Qiu and G. F. Sterman, Nucl. Phys. **B378**, 52 (1992).
[43] Z. B. Kang, Phys. Rev. D **83**, 036006 (2011).
[44] J. C. Collins, Phys. Lett. B **536**, 43 (2002).
[45] C. J. Bomhof, P. J. Mulders, and F. Pijlman, Phys. Lett. B **596**, 277 (2004).
[46] J. Collins and J. W. Qiu, Phys. Rev. D **75**, 114014 (2007).
[47] J. Collins, arXiv:0708.4410.
[48] T. C. Rogers and P. J. Mulders, Phys. Rev. D **81**, 094006 (2010).
[49] D. Boer, P. J. Mulders, and C. Pisano, Phys. Lett. B **660**, 360 (2008).
[50] D. Boer, P. J. Mulders, and C. Pisano, Phys. Rev. D **80**, 094017 (2009).
[51] U. D'Alesio, C. Pisano, and F. Murgia, Phys. Rev. D **83**, 034021 (2011).
[52] F. Gelis, T. Lappi, and R. Venugopalan, Phys. Rev. D **78**, 054019 (2008); H. Fujii, F. Gelis, and R. Venugopalan, Nucl. Phys. A **774**, 793 (2006).
[53] I. Balitsky, arXiv:hep-ph/0101042.
[54] F. Dominguez, B. W. Xiao, and F. Yuan, Phys. Rev. Lett. **106**, 022301 (2011); B. W. Xiao and F. Yuan, Phys. Rev. D **82**, 114009 (2010).
[55] B. I. Abelev *et al.* (STAR Collaboration), Phys. Rev. Lett. **99**, 142003 (2007).
[56] A. Adare *et al.* (PHENIX Collaboration), Phys. Rev. D **82**, 012001 (2010).
[57] A. Adare *et al.* (PHENIX Collaboration), Phys. Rev. D **82**, 112008 (2010).
[58] A. Adare *et al.* (PHENIX Collaboration), Phys. Rev. D **82**, 072001 (2010).
[59] J. C. Collins, D. E. Soper, and G. F. Sterman, Nucl. Phys. **B261**, 104 (1985); J. C. Collins, D. E. Soper, and G. F. Sterman, Nucl. Phys. **B308**, 833 (1988).
[60] A. Bacchetta, M. Diehl, K. Goeke, A. Metz, P. J. Mulders, and M. Schlegel, J. High Energy Phys. 02 (2007) 093.
[61] N. G. Stefanis, I. O. Cherednikov, and A. I. Karanikas, Proc. Sci., C2010 (**2010**) 053.
[62] B. U. Musch, Ph.D. thesis, Technische Universitat Munchen, Physik Department, 2010, arXiv:0907.2381.
[63] B. U. Musch, P. Hagler, J. W. Negele, and A. Schafer, Phys. Rev. D **83**, 094507 (2011).
[64] J. C. Collins and A. Metz, Phys. Rev. Lett. **93**, 252001 (2004).
[65] T. Becher and M. Neubert, arXiv:1007.4005.
[66] J. C. Collins and D. E. Soper, Nucl. Phys. **B197**, 446 (1982).
[67] A. D. Martin, W. J. Stirling, R. S. Thorne, and G. Watt, Eur. Phys. J. C **63**, 189 (2009).

[68] J. A. Paradiso, Ph.D. thesis, Massachusetts Institute of Technology, 1981; D. Antreasyan *et al.*, Phys. Rev. Lett. **47**, 12 (1981).
[69] G. Moreno *et al.*, Phys. Rev. D **43**, 2815 (1991).
[70] A. S. Ito *et al.*, Phys. Rev. D **23**, 604 (1981).
[71] F. Abe *et al.* (CDF Collaboration), Phys. Rev. Lett. **67**, 2937 (1991); J. S. T. Ng, Ph.D. thesis, Harvard University [Report No. HUHEPL-12, 1991].
[72] B. Abbott *et al.* (D0 Collaboration), Phys. Rev. D **61**, 032004 (2000).
[73] A. A. Affolder *et al.* (CDF Collaboration), Phys. Rev. Lett. **84**, 845 (2000).
[74] A. Airapetian *et al.* (HERMES Collaboration), Phys. Lett. B **684**, 114 (2010).
[75] A. Airapetian *et al.* (HERMES Collaboration), Phys. Lett. B **562**, 182 (2003).
[76] A. V. Konychev and P. M. Nadolsky, Phys. Lett. B **633**, 710 (2006).
[77] http://www.pv.infn.it/ radici/FFdatabase/.
[78] S. Kretzer, Phys. Rev. D **62**, 054001 (2000).
[79] B. A. Kniehl, G. Kramer, and B. Potter, Nucl. Phys. **B582**, 514 (2000).
[80] L. Bourhis, M. Fontannaz, J. P. Guillet, and M. Werlen, Eur. Phys. J. C **19**, 89 (2001).
[81] G. Aad (ATLAS Collaboration), J. High Energy Phys. 12 (2010) 060.
[82] A. Bacchetta, D. Boer, M. Diehl, and P. J. Mulders, J. High Energy Phys. 08 (2008) 023.
[83] P. M. Nadolsky, C. Balazs, E. L. Berger, and C. P. Yuan, Phys. Rev. D **76**, 013008 (2007).
[84] S. Catani and M. Grazzini, Nucl. Phys. **B845**, 297 (2011).
[85] D. Boer, S. J. Brodsky, P. J. Mulders, and C. Pisano, Phys. Rev. Lett. **106**, 132001 (2011).
[86] F. Dominguez, C. Marquet, B. W. Xiao, and F. Yuan, Phys. Rev. D **83**, 105005 (2011).
[87] J. C. Collins and T. C. Rogers, Phys. Rev. D **78**, 054012 (2008).
[88] D. Binosi and L. Theussl, Comput. Phys. Commun. **161**, 76 (2004); D. Binosi, J. Collins, C. Kaufhold, and L. Theussl, arXiv:0811.4113.